INSTITUTO POLITÉCNICO DE BRAGANÇA
Escola Superior de Tecnologia e Gestão

Design and Synthesis of Molecularly Imprinted Polymers to Target Olive Leaf Secoiridoids

Ayssata Patrícia da Costa Leocádia Vaz d'Almeida

Thesis presented to the **Escola Superior de Tecnologia e Gestão – Instituto Politécnico de Bragança**, under the guidance and supervision of the **Professor Doctor Rolando Carlos Pereira Simões Dias**, presented to the institute itself as a requirement for obtaining the **master's degree in Chemical Engineering**.

NOVEMBER, 2022

ACKNOWLEDGMENT

I would like to express my deepest gratitude to my advisor, professor Doctor Rolando Carlos Pereira Simões Dias has been an ideal teacher, mentor, and thesis supervisor, offering advice with a perfect blend of insight and humour. I'm proud of, and grateful for my time working with him. I'd like to recognize the invaluable assistance of Catarina Gomes and thank her for the numerous times she has been predisposed to guide me. Amir Bzainia for his willingness to explain and argue different topics. While I was working in the laboratory both Cláudia Martins and Cristina Nogueira provided a very easy to work environment. Thank you for taking the time to proofread the drafts of this thesis. My heartfelt appreciations to all of you.

Countless people supported my effort in this essay, I am indebted to several colleagues who have helped me in many tasks over these years. In particular, I'd like to thank Maria João for always having such a pleasant aura. Most importantly, I am grateful for my mother's unconditional, unequivocal, and loving encouragement, and a special thank you to my father for his role in making it possible for me to be here today.

I would like to thank my better half for being so supportive while I was working, thank you for your many constructive suggestions, for your emotional support, for being so understanding, and for being such a great friend.

We acknowledge the support through the OLEAF4VALUE project. This project has received funding from the Bio-Based Industries Joint Undertaking under the European Union's Horizon 2020 research and innovation programme under grant agreement nº 101023256.

To my grandmother, Cecília Riôa.

ABSTRACT

The purification and concentration of bioactive compounds have become more relevant over time, as these compounds have applicability both at laboratory and industrial scale. Despite their importance, our knowledge of techniques to efficiently isolate these bioactive compounds is impecunious. At this juncture, molecularly imprinted polymeric materials (MIPs) capable of selective recognition and capture of secoiridoids present in olive leaves were synthesized. The combination of different monomers and polymerisation techniques has given rise to twenty-one molecularly imprinted materials comprising different morphologies. These materials were characterized and applied as adsorbents in solid phase extraction (SPE) cartridges, tests performed also included the commercial resins REILLEX402, REILLEX425, XAD4, XAD7HP, and DAX8, where preliminary adsorption studies corroborated the reported high-performance of materials containing the functional monomer 4-vinylpyridine (4VP) in both organic solvents and hydroalcoholic mixtures. In addition to oleuropein, tyrosol, vanillin, quercetin, verbascoside, vanillic acid, and caffeic acid were also considered as template molecules, as they tend to appear in olive leaf extracts. By using an olive leaf extract in adsorption/desorption cycles, fractionation and concentration of phenolic compounds present in the initial extract were achieved, thus luteolin-enriched fractions were obtained. The obtained results indicate that although different MIPs have been successfully synthesized, for the desired purpose the adsorbents MIP3 and MIP7 are the most adequate and they can be used in sequence with Reillex402 to optimize the purification/concentration process of the compounds present in the extracts.

Keywords: Molecular imprinting, polyphenols, secoiridoids, olive leaves extracts, fractionation, bio-circular economy.

RESUMO

A purificação e concentração de compostos bioativos tem se tornado mais relevante aos longos dos tempos, dada a sua aplicabilidade tanto a nível laboratorial quanto industrial. Apesar de sua importância, o conhecimento de técnicas para isolar eficientemente esses bioativos é escasso. Nesta conjuntura, foram projetados e sintetizados materiais poliméricos com impressão molecular capazes de reconhecimento seletivo e captura de secoiridóides presentes em folhas de oliveira. A combinação de diferentes monómeros e técnicas de polimerização deu origem a vinte e um materiais molecularmente impressos que compreendem diferentes morfologias. Esses materiais foram caracterizados e usados como adsorventes em cartuchos de extração em fase sólida (SPE), os testes realizados incluíram também as resinas comerciais REILLEX402, REILLEX425, XAD4, XAD7HP e DAX8, onde, estudos preliminares de adsorção corroboraram o elevado desempenho reportado de materiais contendo o monómero funcional 4-vinilpiridina (4VP) tanto em solventes orgânicos como em misturas aquosas. Para além da oleuropeína, foram também considerados como molécula molde o tirosol, a vanilina, a quercetina, o verbascosideo, o ácido vanílico, e o ácido cafeico, visto que estes têm tendência a aparecer nos extratos da folha da oliveira. Ao considerar extratos de folhas de oliveira em ciclos de adsorção/dessorção alcançou-se fracionamento e concentração de compostos fenólicos existentes no extrato inicial, dessa forma obteve-se frações enriquecidas em luteolinas. Os resultados obtidos indicam que embora diferentes MIPs tenham sido sintetizados com sucesso, para a finalidade desejada os materiais MIP3 e MIP7 são os que mais se adequam, podendo esses serem usados de forma sequencial em conjunto com o REILLEX402 de modo a otimizar o processo de purificação/concentração dos compostos presentes nos extratos.

Palavra-chave: Impressão molecular, polifenóis, secoiridoides, extratos de folhas de oliveira, fracionamento, economia bio-circular.

PREFACE

Extracting analytes from more complex matrices, as is the case of plant matrices, always becomes a challenge, many techniques are used, and among them solid phase extraction (SPE) stands out. SPE is based on the difference of affinity between the stationary phases (adsorbent) and the analyte (sorbent). This technique is limited by the possibility of coelution of the analyte with the other constituents of the sample. Therefore, there is an urgent need to synthesize adsorbents that guarantee greater selectivity.

It is intended with this topic to explore polymerization parameters such as initiation type and functional monomer and their best suitability for synthesis aiming sustainability and reproducibility. In this work some synthesis strategies of molecularly imprinted materials for selective capture and concentration of secoiridoids present in olive leaves were implemented, insertion/manipulation of functionality by hybridization was also explored. The resulting materials were employed in SPE cartridges for evaluation of their retention capacity and selectivity.

The present work is summarised in 7 chapters. Chapter 1 begins by introducing the family of target compounds in this work, presenting as the source for obtaining these bioactive compounds, the olive leaves. Besides showing the methods adopted for extraction. Chapter 2 presents a summary of the available bibliography about the polymerization processes. Chapter 3 outlines the available bibliography on molecular imprinting and the different variables of this process. In chapter 4, the reagents and equipment used in this work are described. In chapter 5 the strategies for the preparation of the MIPs and NIPs are presented, in this is included the experimental part (synthesis, regeneration, characterization, and application in SPE), the results, and the discussion. In chapter 6, some key points in this thesis have been selected and addressed in the general conclusion, and some future perspectives based on this work are also suggested. Chapter 7 presents the bibliographical references. In the end, a set of appendices that support the accomplished work are displayed.

CONTENTS

LIST OF FIGURES

LIST OF TABLES

LIST OF GRAPHICS

LIST OF APPENDICES

CHAPTER 1. INTRODUCTION

Olea europaea, Oleaceae, belongs to the Oleoaceae family and the genus *Olea*, composed of 30 species. The olive tree, *Figure 1*, differs from other fruit species due to its longevity and rusticity, which can develop in sub-arid climates and very poor soils [1]. The medicinal properties of the olive leaf have been reported since antiquity, records show biblical references to its use [2]. The cultivation of the olive tree, as well as the use of its leaves in traditional medicine, is originally popular in the Mediterranean region [3], namely, Greece, Spain, Italy, France, Turkey, Israel, Morocco, and Tunisia.

Figure 1: Olive Trees.

Olive leaves have in their composition, several potentially bioactive compounds that can have antioxidant, antihypertensive, antiatherogenic, anti-inflammatory, hypocholesterolemic, hypoglycemic and hypolipidemic properties [2,3].

Both traditionally and widely, olive and olive leaves (a by-product) have been used over time in food and to prevent and treat diseases. Aiming at environmental and economic sustainability, as well as improving general health, there is a need to investigate natural materials that can replace synthetic ones. For this reason, extracts from vegetable matrices have received particular attention from the food, cosmetics, and pharmaceutical industries. It is known that the bioactivity of the extracts obtained from the olive by-products (leaves, pomace) in medicine and food industry is due to the presence of bioactive compounds known as polyphenols that can prevent oxidative damage [2].

The term “olive leaves” often times may refer to a mixture of leaves and branches from both the pruning of olive trees and the harvesting and cleaning of olives. The production of olive leaves from pruning is about 25 kg per olive tree per year, and the

Figure 2: Olive leaves of Cobrançosa variety.

leaves represent 10% of the weight of the collected olive tree [3,4]. In most cases, the by-products of the cultivation and processing of the olive tree, in particular the leaves, *Figure 2*, do not receive a final application other than burning or grinding along with the rest of the olive pruning by-products. These removal, storage, and disposal steps, in addition to having costs for producers, can seriously impact the environment if not properly controlled [4].

1.1. Polyphenols

Polyphenols are secondary metabolites of plants, they are naturally occurring compounds found largely in the fruits, vegetables and cereals and are generally involved in defence against ultraviolet radiation or aggression by pathogens. Polyphenols are known to contribute to the bitterness, astringency, colour, flavour, odour, and oxidative stability of foods (e.g. olive oil). There is an increasing scientific interest because of their possible beneficial effects on human health, long term consumption of diets rich in plant polyphenols may offer some protection against development of cancers, cardiovascular diseases, diabetes, osteoporosis, and neurodegenerative diseases [5].

1.1.1. Polyphenols present in olive leaves

More than 8000 polyphenolic compounds have been identified in various plant species. As the name indicates, those compounds have in their structure at least two hydroxyl/phenolic groups. Polyphenols encompass various classes and are constituted in many heterogeneous structures that range from simple molecules to highly polymerized compounds, the main classes include phenolic acids, flavonoids, stilbenes and lignans [5]. *Figure 3* illustrates the different groups of polyphenols found in olive leaves and their chemical structures.

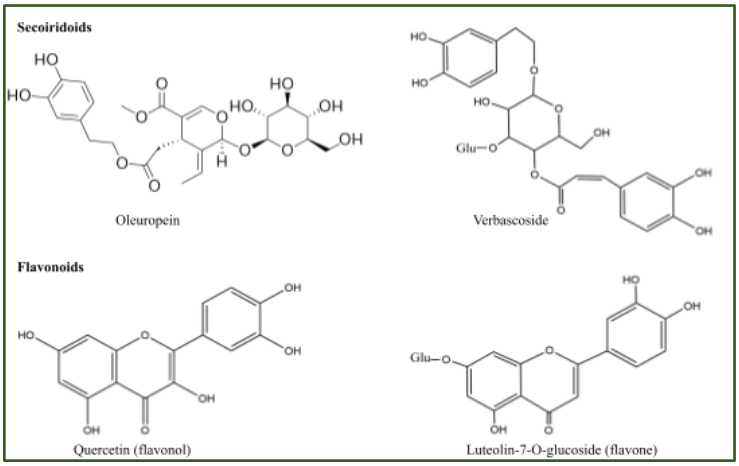

Figure 3: Chemical structure of some polyphenols groups.

Phenolic acids -- are further divided into hydroxyl benzoic and hydroxyl cinnamic acids. Caffeic acid, gallic acid and ferulic acid are some common phenolic acids.

Flavonoids -- are most abundant polyphenols in human diet and share a common basic structure consist of two aromatic rings, which are bound together by three carbon atoms that form an oxygenated heterocycle. Quercetin, myricetin and catechins are some most common flavonoids.

Stilbenes -- contain two phenyl moieties connected by a two-carbon methylene bridge. Most stilbenes in plants act as antifungal phytoalexins, compounds that are synthesized only in response to infection or injury. The most extensively studied stilbene is resveratrol, found largely in grapes.

Lignans -- are diphenolic compounds that contain a 2,3-dibenzylbutane structure that is formed by the dimerization of two cinnamic acid residues.

1.1.2. Oleuropein

In comparison with olive oil, the olive leaves contain higher amounts of polyphenols, for example, the amount of oleuropein, which is the most abundant phenolic compound ranges from 0.005% and 0.12% in olive oil while in olive leaves it ranges between 1 and 14% [6]. In the case of the olive tree (and other plants in general), the existent polyphenols are a consequence of the reactivity to pathogen attack and the response to insect injuries. The oleuropein is the most abundant phenolic compound in

olive leaves, followed by hydroxytyrosol, luteolin-7-glucosides, apigenin-7-glucosides and verbascoside. The hydroxytyrosol is the precursor of the oleuropein, while the verbascoside is a conjugated glucoside of hydroxytyrosol and caffeic acid [3,6]. *Figure 4* illustrates the chemical structure of oleuropein.

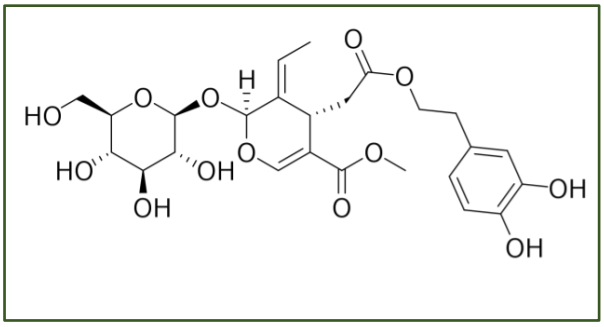

Figure 4: Oleuropein molecular structure.

Oleuropein is a basic phenolic compound found in olive leaf and the reason of the characteristic bitter taste of olive cultivars, it is present in high amounts in unprocessed olive fruit and leaves, while hydroxytyrosol is more abundant in the processed olive fruit and olive oil.

The decrease in the concentration of oleuropein and consequent increase in the concentration of hydroxytyrosol occurs due to chemical and enzymatic reactions that take place during maturation of the fruit or due to olive processing (e.g., oil production) [3].

It is reported that oleuropein (given by ingestion or intravenously) reduces blood pressure and dilates coronary arteries. *In vitro*, oleuropein has been found to inhibit the oxidation of cholesterol carried by low-density lipoproteins (LDL - known as "bad cholesterol"). Oxidation of LDL cholesterol can lead to symptoms or the development of heart disease. Studies point to the bacterial activity of oleuropein, which under certain conditions converts to elenolic acid. *In vitro* analyses with this acid have demonstrated bactericidal activity against various species, such as *Staphylococcus aureus* and *Bacillus subtilis* [7,8].

1.1.3. Methods for extraction and purification

The choice of the method of extraction and purification is considered critical in research involving natural products. Moreover, extracts composition is strongly

dependent on their production conditions, namely the kind(s) of solvent used, time, and temperature. Therefore, the development of tailored adsorbents is a key point aiming at the design of efficient sorption/desorption processes to target polyphenols [9,10]. The methods adopted for the extraction are followed described.

a) Ultrasound

The ultrasound-assisted extraction (UAE) creates and collapses cavitation of small bubbles in the solvent due to the passage of ultrasound waves, which allows greater penetration of the solvent within the material increasing the surface area, hence favouring extraction [9].

The advantages of this technique are reducing the extraction time (cavitation accelerates chemical reaction by improving mass transport), reduction in the volume of chemical solvents (comparatively to Soxhlet for instance). On the other hand, possible damage may be caused, the UAE process favours the dilation and hydration of the plant material leading to the enlargement of the pores of the cell wall causing the increase in swelling and mass transfer ratio and, eventually, to cell wall breakdown [9].

b) Supercritical fluid

The most used solvent for extraction in this technique is carbon dioxide (CO_2), which is inert, non-flammable, and does not harm the environment, even though this substance has a nonpolar nature, making difficult to use in extracting polar compounds, its use count as a method environmentally safe and efficient. Supercritical fluids have a similar density to ordinary fluids and many substances have good solubility in them. Meanwhile, it also keeps the transfer properties and easy penetration characteristics of gases. Small changes in temperature or pressure near the critical point will cause a very significant change in the density of the supercritical fluid, making it easy to separate solvent and extract [9,11].

The main advantages of supercritical fluid extraction (SFE) are the use of low temperatures, low energy consumption, low levels of degradation of chemical

compounds, the possibility of operational changes during extraction. The main disadvantage is that with the use of high pressures, expensive equipment is required, increasing the cost of the final product [9].

1.2. Molecular Recognition

Molecular recognition plays a critical role in numerous living systems, protein-based receptors, nucleic acids, enzymes, and antibodies are outstanding examples of biological materials that have high molecular binding selectivity [12].

Nowadays, molecular imprinting theory is attractive in many scientific fields, however, despite the growing interest in this technology being recent, the concept is not. At the beginning of the current century, a lot of effort was devoted into the development of new materials for application in chromatography. Soviet scientist M.V. Polyakov conducted a series of investigations and tests with silica for use in chromatography, in short, Polyakov realized that when silica was placed in a desiccator, containing a beaker with one of the additives (benzene, toluene or xylene), the extent of adsorption of the different additives was shown to be dependent on the structure of the additive present during the drying process [13].

In 1949, Frank Dickey (a senior student of Linus Pauling) published the results of experiments carried out with silica gels obtained in the presence of dyes, Dickey observed that, after removal of the template dye, the silica preferentially bound to this dye compared to others [13].

CHAPTER 2. SYNTHESIS METHOD

The first papers published on free radical polymerization (FRP) are from the 1940s and 1950s, but even in the 1930s the applications of this technique rapidly propelled it to a commercial scale for the manufacturing of various oil-derived polymeric materials. Nowadays, FRP is the chosen method to produce several well-known commodities such as polystyrene, polyethylene, polybutadienes, polyvenylacetates, and others that improve everyday life.

This method is almost solely used to prepare polymer from monomers of the general structure $CH_2 = CR_1R_2$ since the reaction does not require high-purity reactants and rigorous exclusion of moisture, air, and other impurities, plus, it can be performed under mild reaction conditions (e.g. ambient temperatures and atmospheric pressures), in bulk or in solution, the molecular weight distribution characteristic of FRP is, however, not optimal for some polymer applications. For ecological and economic reasons, industries are moving towards bio resourced polymers, and in the 1990s the concept of reversible deactivation, known as controlled/living RP technic was introduced, the chance of manipulating and controlling the termination reaction brings new possibilities for vinyl polymers [14,15].

2.1. Free Radical Polymerization

The most conventional mechanism of free radical polymerization includes three well-defined reaction steps: initiation, propagation, and bimolecular termination. Free radicals are highly reactive species that possess an unpaired electron, produced physically (thermoexcitation, radiation) or chemically (oxidation-reduction, addition, etc.) by the homolytic dissociation of covalent bonds with a short lifetime [15,16].

2.1.1. Initiation

The initiation step is considered to involve two reactions. The first being the production of free radicals, and the second part of the initiation involves the addition of this radical to the first monomer molecule to produce the chain-initiating radical.

Azo and peroxide initiators are commonly used in molecular imprinting (benzoyl peroxide (BPO) and 2,2'-azo-bis-isobutyrylnitrile (AIBN)), for the azo initiator, the free radicals are generated by UV radiation at the wavelength for maximum absorption, or thermally at a temperature providing a suitable rate of decomposition, note that (1) if the rate is too high, a large concentration of reactive centers will be generated leading to premature termination and low molecular weights and (2) if it is too low, the polymerization will not reach completion at a reasonable time frame [17].

2.1.2. Propagation

Propagation consists of the growth of the first radical by rapid successive additions of large numbers of monomer molecules to the active centre. Each addition will create a new radical that has the same identity as the previous, except that it is larger by one monomer unit [16,17].

2.1.3. Termination

In theory the propagation step would continue until all monomers are consumed. However, pairs of radicals tend to react with each other and thus annihilate their activities. Termination most common mechanisms, combination or disproportionation, involve bimolecular reaction of the growing polymer chain.

- Combination (coupling), two growing polymer chains react with each other forming a single nonreactive polymer chain:

$$Mx\cdot + My\cdot \rightarrow M_{x+y} \qquad \text{(Eq.2-4a)}$$

- Disproportionation, a hydrogen atom is transferred from one radical to the other resulting in two polymers, one with a saturated end and the other with an unsaturated end and each with an initiator fragment:

$$Mx\cdot + My\cdot \rightarrow Mx + My \quad \text{(Eq.2-4b)}$$

2.2. Controlled Radical Polymerization

Szwarc defined “live” polymerization as one characterized by a process of chain growth exempt of interruption reactions, such as chain termination or transfer. However, there is a difference between “live” and “controlled” polymerization, “live” polymerization occurs in the total absence of termination or chain transfer reactions, and in “controlled” polymerization these reactions are minimized. Reversible addition-fragmentation chain-transfer (RAFT) polymerization and atom transfer radical polymerization (ATRP) are the two most common controlled radical polymerization methods, which differ from each other as RAFT is based on the transfer of activity between polymer chains bearing dithioester moieties and not on the reversible deactivation of growing polymer chains [18].

2.3. Polymerization techniques

a. Polymerization by precipitation

Precipitation polymerization starts from a homogeneous mixture of monomer, initiator, and inert solvent. During the polymerization process, the growing polymer chains phase-separate from the continuous medium. One disadvantage is that the resulting polymer has to be separated from the reaction system [19].

b. Suspension Polymerization

This polymerization technique enables polymer particles to be obtained as spherical beads and hence this polymerization technique is also known as bead or pearl polymerization [18], suspension polymerization is one of the simplest and most common approaches for the production of MIP beads. This technique involves suspension in either water or perfluorocarbon. Both procedures can produce high-quality MIP beads, but the drawback of the former process is that water is incompatible with most non-

covalent imprinting procedures, on the other hand liquid fluorocarbons are fairly expensive [20].

CHAPTER 3. MOLECULAR IMPRINTED POLYMERS

Molecular imprinted polymers (MIPs) are synthetic crosslinked organic polymers that holds specific cavities designed for a target molecule, the template. These materials oftentimes are designated as artificial antibodies, or as plastic antibodies due to their akin ability to recognize and bind the target analytes selectively, as antibodies do. In comparison to antibodies, MIPs are reported to be more stable to pH, temperature, and organic solvents, have high mechanical strength, low cost, reusability, and they are easy to make [21,22], *Figure 5* presents a general schematisation of the synthesis process.

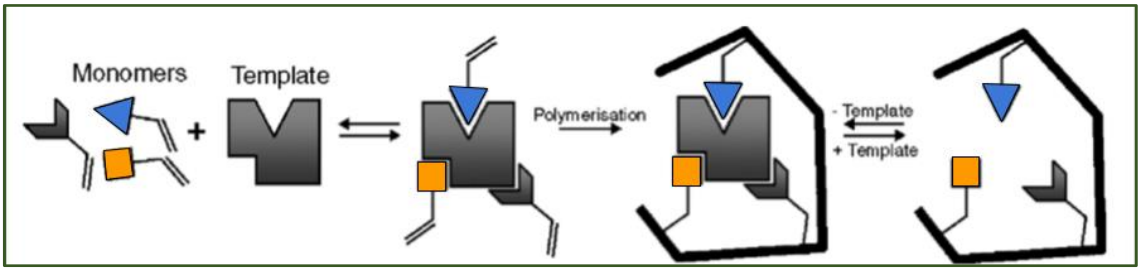

Figure 5: Schematic generalisation of the molecular imprinting process. Adapted from [23].

Substantially, three approaches currently exist to generate high fidelity imprinted sites, these are distinguishable by the nature of the linkage during synthesis and rebinding [23], being them, the covalent, the non-covalent, and the combination of the two previous ones, the semi-covalent.

3.1. Covalent Molecular Imprinting

It is the first example of molecular imprinting and was introduced by Wulff and Sarhan. In this approach, the template molecule covalently binds to the functional monomer prior to the polymerization step. This bond needs to be relatively easy to break in order to allow cleavage of the template molecule post polymerization. When polymerization occurs, a polymer is formed that contains the template molecule, to obtain the MIP, it is first necessary to extract the template from the polymeric matrix, since the synthesis is via covalent interaction, these bonds must be broken, and, in most cases, chemical cleavage is necessary [13,23-25]. *Figure 6* presents a general schematisation of the covalent molecular imprinting.

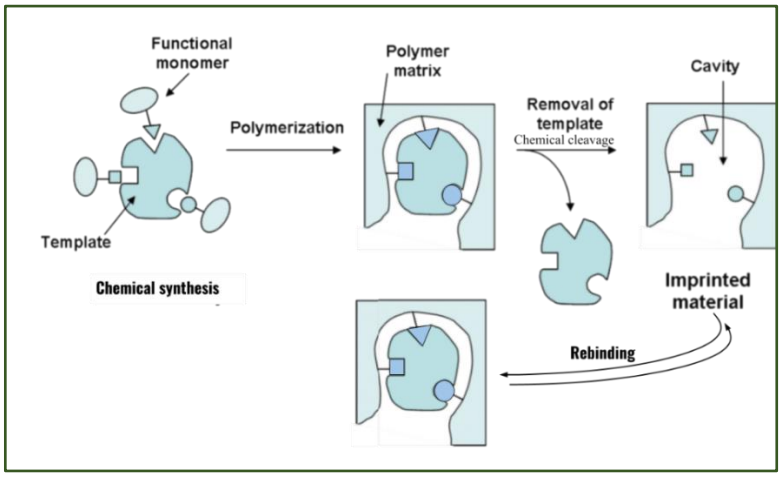

Figure 6: Schematic representation of the covalent molecular imprinting. Adapted from [23,26]

This synthesis method presents the following advantages: stability of the monomer/template complex, known stoichiometry, which favours the recovery of the template, more selective sites, i.e., there is a reduction in the number of non-selective sites due to the presence of strong interactions between the template molecule and the functional monomer. On the other hand, there is a limited number of template molecules (TM) and functional monomers (FM) that satisfy such criterion, the applicability of the method ends up being restricted to TM that belong to the category of alcohols, aldehydes and ketones, amines, and carboxylic acids [24,26].

3.2. Non-Covalent Molecular Imprinting

The second milestone in organic polymer molecular imprinting technology occurred in 1981 when Arshady and Mosbach prepared an organic MIP based on the process that is now called non-covalent imprinting [26]. This approach is based on the reversibility of multiple non-covalent interactions between the template and the functional monomer, here, the monomers must be selected to allow non-covalent bonds (such as hydrogen bonds, dipole-dipole bonds, ionic interactions, π–π and/or hydrophobic interactions) with the TM [13]. Before polymerization functional monomer and template molecule are self-assembled by simple dissolution in a suitable solvent, followed by the addition of the crosslinker, which initiates polymerization, extraction of the template molecule from the polymer matrix is achieved by washing with convenient solvents [13,26].

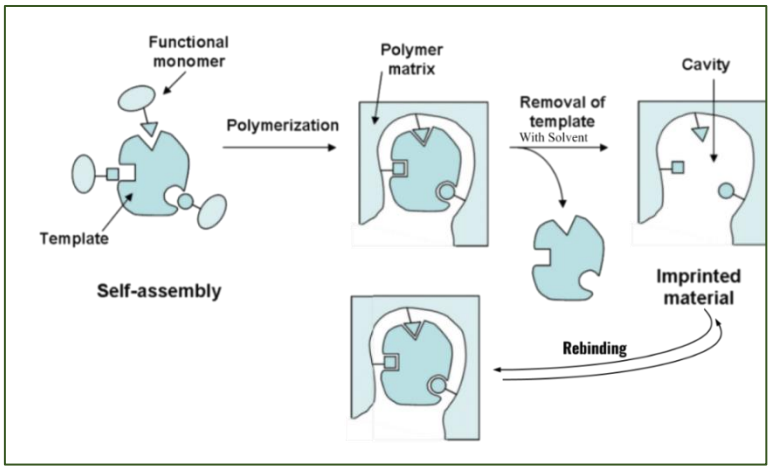

Figure 7: Schematic representation of the non-covalent molecular imprinting. Adapted from [23,26]

The non-covalent imprinting approach, *Figure 7*, seems to hold more potential for the future of molecular imprinting owing to the vast number of compounds, even biological compounds, which are capable of non-covalent interactions with functional monomers, without mentioning the simplicity of execution, the possibility of using the resulting MIP directly in separation processes with high affinity and selectivity (stationary phase in chromatography), a greater diversity of functionalities can be inserted within the MIP binding sites, implying greater flexibility in the application of MIP for different analytes and still easier elution. However, non-covalent systems cause

binding site heterogeneity. As the non-covalent bonds tend not to be strong, an excess of FM in relation to TM is necessary to favour the formation of the model monomer-template complex, this results in the random incorporation of the FM in the polymer matrix, which tends to cause the formation of non-specific binding sites [6,13].

Other limits to the non-covalent molecular imprinting are set by the peculiar molecular recognition conditions. Most of the fact, the formation of interactions between monomers and the template are stabilized under hydrophobic environments, while polar environments disrupt them easily. Another limit is represented by the need for several distinct points of interaction: some molecules characterized by a single interacting group, such as an isolated carboxyl, generally give imprinted polymers with very limited molecular recognition properties, which have little interest in practical applications [26].

The non-covalent approach is still by far the most widely used in MIP synthesis. Some of its drawbacks can be outgrown by the use of stoichiometrically associating monomer-template systems. This has resulted in a range of receptors exhibiting high capacity and effective recognition [23].

3.3. Semi-Covalent Molecular Imprinting

Whitcombe et al. described in 1995 a hybrid approach, semi-covalent imprinting, this appears to combine the advantages of both processes described above and thus optimize the molecular imprinting process [26]. The semi-covalent designation, *Figure 8*, integrates all imprinting methods in which, in the polymerization step, is used a template structure, which will establish a covalent or partially covalent bond with the functional monomers, and in which, in the analyte rebinding step, it is established a bond of a non-covalent nature. In simplified form, a methacrylate ester of the template molecule is copolymerized with the monomeric mixture that will form the polymer matrix. The template molecule is subsequently removed by hydrolysis. Its rebinding (in non-esterified form) by the polymer is due to the interaction of its hydroxyl group(s) with the methacrylate groups present in the recognition sites [26].

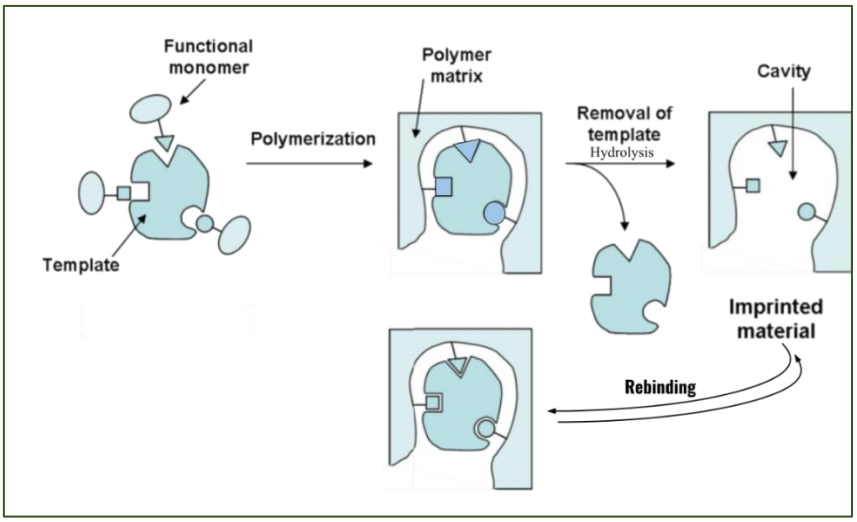

Figure 8: Schematic representation of the semi-covalent molecular imprinting. Adapted from [23]

This new approach, compared to the method described by Arshady and Mosbach, has valuable advantages, it dispenses the use of excess FM during the synthesis phase, thus, solving the issue of low selectivity due to the increase in specific sites. There is also greater uniformity of binding sites and better TM removal at the end of the process, which avoids residual elution after the rebinding steps with sample elution [25]. The disadvantage is that the molecular recognition process can be compromised due to TM hydrolysis because in the establishment of hydrogen bonds (in the rebinding step) the stereochemical requirements of an acid and an alcohol are very different from those of the corresponding ester [25,26].

3.4. Variables of the MIPs Synthesis Process

The components of a Molecularly Imprinted Polymer are template, functional monomer, crosslinker, solvent, and initiator. Several things determine the success of a MIP, but its components and the interaction between template-monomers are the most critical factors. When making MIPs, a functional monomer is preferred over an ordinary monomer because a functional monomer contains a Y functional group that can interact with template molecules via hydrogen bonding, dipole-dipole, and ionic interaction to produce a template-monomer complex. The complex is then fixed in an excess

crosslinking agent, and a three-dimensional polymer network is formed. After the polymerization process, template molecules are removed from the polymer using a solvent, resulting in selective complementary polymer-template bonds. Thus, the optimization of the parameters involved in the synthesis is essential for the making of MIPs [24,27].

3.4.1. Template (Imprint molecule)

In all molecular imprinting processes, the template is of critical role, its molecular structures determine the type of functional monomer to be used in the synthesis therefore the template molecule must be evaluated for the presence of functional groups capable of binding to functional monomers to form a stable complex. One way to check the stability of the formed complex is to evaluate the binding energy, the lowest binding energy indicates high complex stability [24,27].

On the other hand, this molecule must not have groups that accelerate or delay polymerization (for example, the thiol or hydroquinone group), as well as polymerizable groups that can promote its insertion into the polymeric network and, consequently, the non-formation of recognition sites [24,26].

In terms of polymerization compatibility, the template must be chemically inert under the polymerization conditions. If the template exhibits free-radical reactions or unstable reactions under the conditions of polymerization, alternative imprinting strategies should be used, for example its replacement by a structural analogue [24].

The size of the template molecule influences the selectivity of MIPs, most routine MIP were using small organic molecules as template. MIPs for large molecules are demonstrably less selective, due to the formation of specific “large” sites, which allow the entry of other small molecules present in the sample. Although specially adapted protocols have been proposed for larger organic compounds, e.g., proteins, cells, imprinting of much larger structures are still a challenge. The main reason is the fact

that larger templates are less rigid and thus do not facilitate creation of well-defined binding cavities during the imprinting process [24,28].

Furthermore, the secondary and tertiary structure of large biomolecules such as proteins may be affected when exposed to the thermal or photolytic treatment involved in the synthesis of imprinted polymers. Rebinding is also more difficult, since large molecules such as peptides and proteins do not readily penetrate the polymer network for reoccupation of binding pockets [28].

Some works present an alternative for the recognition of large molecules such as proteins, in these, the MIP is synthesized for an amino acid sequence present in the molecule and the recognition of the protein occurs indirectly to the recognition of the peptide [24].

3.4.2. Functional Monomer

The functional monomers are responsible for the interactions of chemical bonds in the imprinted sites, so the choice of monomer should be made according to the nature of the template molecule, thus, it is important to combine the functional groups of the template with the functional groups of the monomer in a complementary way, to favour the formation of the complex, for example, template molecules that have basic functional groups interact more easily with monomers that contain acidic groups [24,27].

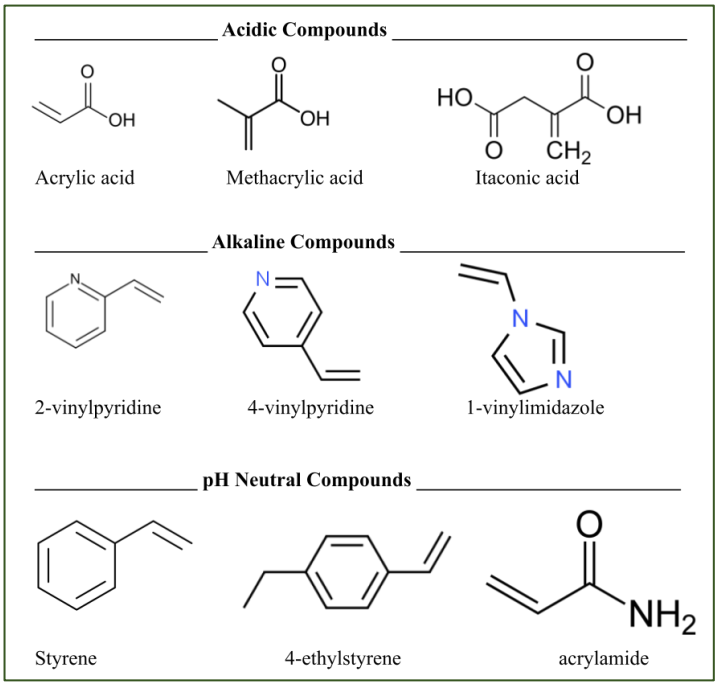

Figure 9: Chemical structure of functional monomers commonly used.

Three types of functional monomers are most used: (i) acidic compounds, such as

methacrylic acid, (ii) alkaline compounds, such as 4-vinyl pyridine, and (iii) pH neutral compounds, such as styrene. Some typical functional monomers are listed in *Figure 9* [27]. These monomers usually have association constants with the template molecule that are too low to form a stable complex. Therefore, an excess of monomer should be used, usually in the ratio of 4:1 (mole fraction) concerning the template molecule, to shift the equilibrium to the formation of the complex [24].

When mixtures of functional monomers are used, this tends to provide more specific cavities in the polymer so, there is a need to consider the molar ratios that promote the reactivity of the monomers to ensure the occurrence of copolymerization [24,29].

In covalent molecular imprinting, the effects of changing the template to functional monomer ratio are not necessary because the template dictates the number of functional monomers that can be covalently attached, furthermore, the functional monomers are attached in a stoichiometric manner. For non-covalent imprinting, the optimal template /monomer ratio is achieved empirically by evaluating several polymers made with different formulations with increasing template amounts [28].

3.4.3. Crosslinking agent

Crosslinkers in molecular imprinting control the morphology of the polymer matrix, stabilize the imprinted binding sites and impart mechanical stability on the polymer matrix. From a polymerization point of view, high crosslink ratios are generally preferred since they are reported to enable the maintenance of the three-dimensional structure of the polymer to be complementary to the template molecules in size and shape and by that generate materials with adequate mechanical stability [28,30].

Quite some crosslinkers compatible with molecular imprinting are known, and a few of them are capable of simultaneously complexing with the template and thus acting as functional monomers. The ethylene glycol dimethacrylate (EGDMA) has been the most widely employed crosslinker in the synthesis of MIPs due to the formation of

thermally and mechanically stable polymers, because it combines a reactive methacrylate ester with a short spacer, allowing a high number of conformations and a certain degree of rigidity in the resulting polymer, EGDMA thus acts as a structural monomer since it creates a three-dimensional polymeric structure that preserves the functional monomer groups in a fixed position and complementary to the template molecule, ensuring rigidity and stability to the binding sites. Another crosslinker widely used is the trimethylolpropane trimethacrylate (TRIM), since it produces MIPs with high selectivity and with higher loading capacity, then, the choice of crosslinking agent should envision the type of application for the resulting polymer. *Figure 10* shows the chemical structure of the crosslinkers mentioned [24,28,30].

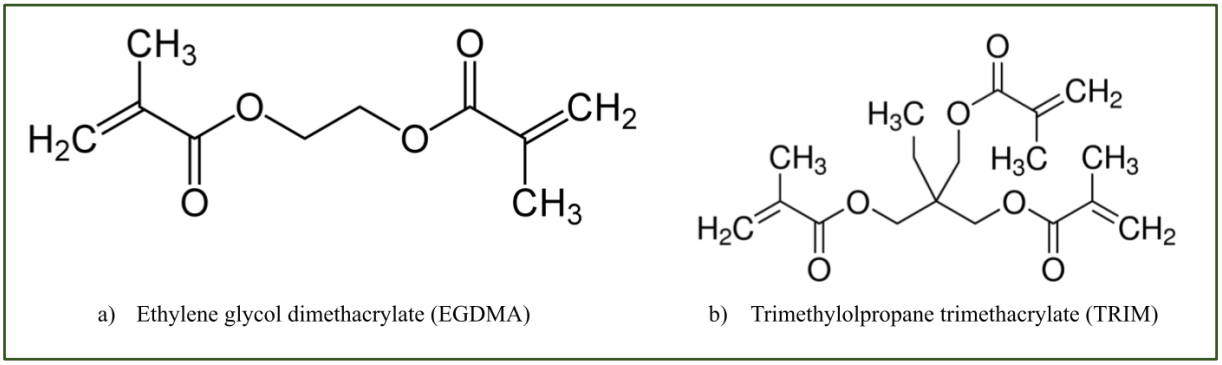

Figure 10: Chemical structure of the crosslinkers: a) Ethylene Glycol Dimethacrylate (EGDMA), and b) Trimethylolpropane Trimethacrylate (TRIM).

3.4.4. Solvent (Porogen)

There are several factors to consider when choosing a porogen, namely: (1) it should be capable of dissolving all the polymer-forming components, (2) it must form a large pore to increase flow-through, and (3) its polarity level must be relatively low to minimize interference with template-monomer interactions. When synthesizing MIPs solvents with lower dielectric constants (ε) such as toluene (ε value 2.38), benzene (ε value 2.28), and acetonitrile (ε value 3.92) is preferable as an aprotic porogenic solvent with a low dielectric constant can increase the binding energy that occurs between template and monomer, a phenomenon that provides MIPs with good selectivity and

affinity due to the high concentration of the template: monomer complex that is formed [31].

The percentage and composition of a porogen are also influential, it is reported that an increase in the amount of the porogen increases the pore volume, average pore diameter, and pore distribution [31]. After the preparation of the polymer and the extraction of the analyte from the selective cavity, the resulting MIP will have a higher affinity for the analyte when it is in a medium similar to that used in the synthesis. Thus, the molecular recognition of a MIP occurs preferably in the same reaction medium in which it was synthesized [24].

3.4.5. Initiator

Radical initiators have the function of generating free radicals that enable the initiation and maintenance of polymerization of the crosslinking agent around the complex functional monomer-template molecule. Once added to the reaction, the initiator undergoes a homolytic break in its structure, triggered by external stimuli such as temperature or UV radiation, to generate the radicals that initiate polymerization. It has been observed that, in general, MIPs are best synthesized over long periods using a low concentration of initiator and low temperature. The choice of initiator must be made based on the physicochemical properties of the template molecule [24,29,30].

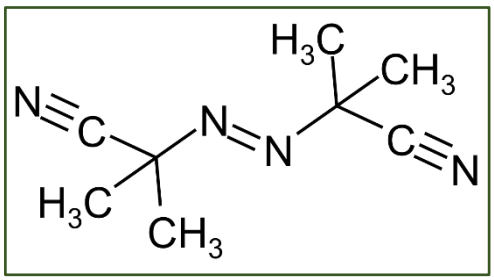

Figure 11: Molecular structure of the initiator 2,2'-Azobis(2-methylpropionitrile) AIBN.

- If the template molecule is photochemically or thermochemically unstable, initiators which can react both photochemically and thermochemically should not be selected. If the interaction occurs by hydrogen bonding, polymerization must take place

at low temperatures, then under these conditions, photochemically active initiators are the most suitable [24,29].

The initiator 2,2'-Azobis(2-methylpropionitrile) (AIBN) can be decomposed by both temperature and photolysis, hence its extensive use in the synthesis of MIPs, other initiators such as, for example, azobisdimethylvaleronitrile (ABDV) and benzoyl peroxide (BPO) can also be used, and the choice of the most suitable one depends on the synthesis temperature to be employed and the analyte (TM). AIBN is employed as a radical initiator when the template molecule is stable at a temperature of approximately 60°C or exposure to UV radiation. The chemical structures of one of the selected polymerization initiators are shown in *Figure 11* [24].

- If present in the reaction medium, oxygen can lead to a decrease of radicals, which impairs polymerization. For this reason, in addition to the variables mentioned above, it is worth mentioning the need to conduct the reaction in the absence of oxygen by means of purging with an inert gas such as nitrogen and argan or by employing an ultrasonic bath [24].

3.5. MIPs Applications

The recent notoriety of MIPs is due to their wide range of potential applications. These materials, primarily used in separation processes (solid phase in SPE), have been attracting interest from researchers thanks to their enhanced characteristics compared to adsorbents, their ease of synthesis, lower price, and much-reported selectivity have generated curiosity of use in various areas such as:

a. Chiral separations by liquid chromatography and capillary electrophoresis as MIPs poses high capabilities in extraction through highly specific micro-cavity binding sites.
b. Biosensors for effluent pre-treatment (capture/recovery of heavy metals, dyes, pesticides, and drugs, etc.), food analysis for residue removal (fluoroquinolones in fish samples, lincomycin residue in pasteurized milk, etc), drug screening and biomedical diagnostics - by using MIPs as biomarkers, MIPs are known as an artificial receptor that has basic capabilities like natural receptors, one of which is the ability to recognize cells, gathering advantages such as high affinity and selectivity and greater temperature stability, MIP as an alternative to antibodies is often used as an analytical method for diagnostic purposes such as breast cancer diagnostics, cardiovascular disease, and dengue fever.
c. In Drug-delivery systems (DDS) the use of MIP as a DDS agent offers several advantages, namely long shelf life, easy preparation, high chemical, physical stability, and low cost, some studies show that MIP nanoparticles, through a physical approach, have the potential to make effective drugs to attack multidrug-resistant cells with the right temperature at the target location [24,27].

CHAPTER 4. MATERIALS AND EQUIPMENT

4.1. Reagents

All reagents used in this study were purchased from commercial vendors and used without further purification. These reagents are displayed in *Table 1*.

Table 1: Reagents used during synthesis and material evaluation.

Reagents	Molecular Form	Chemical Structure	Molecular Weight (g/mol)	Density (g/mL)	Supplier
(3-Aminopropyl) trimethoxysilane (3-AT)	$C_9H_{23}NO_3Si$	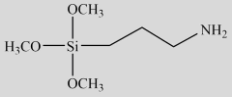	221.37	--	Sigma-Aldrich
1-[3-(Trimethoxysilyl) propyl]urea	$(CH_3O)_3Si(CH_2)_3NHCONH_2$	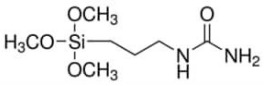	222.31	--	Sigma-Aldrich
2,2'-Azobis[2-(2-imidazolin-2-yl) propane]dihydrochloride (VA044)	$C_{12}H_{24}C_{l2}N_2$	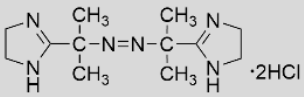	323.27	--	Wako
4VAN-BTPI	$C_{17}H_{14}F_6N_2O$	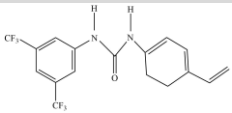	374.28	--	--
4-vinylpyridine (4VP)	$CH_2CHC_2H_2N$	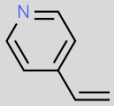	105.14	1.051	Alfa Aesar
Acetonitril (ACN)	CH_3CN	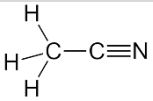	41.05	0.786	Fisher Chemical
Acrylamide (AAm)	C_3H_5NO	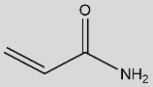	71.08	1.13	Fluka Analytical
Azobisisobutyronitrile (AIBN)	$[(CH_3)_2C]_2N_2$	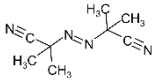	164.21	1.1	Fluka Analytical

Table 1: Continuation of the reagents used during synthesis and material evaluation.

Caffeic acid	$C_9H_8O_4$	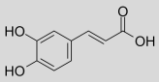	180.16	1.48	Acros Organics
Dimethyl sulfoxide (DMSO)	C_2H_6OS	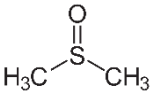	78.13	1.1	Fisher Bioreagents
Dimethylformamide (DMF)	$(CH_3)_2NCH$	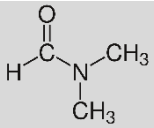	73.09	0.944	VWR chemicals
Divinylbenzene (DVB)	$C_{10}H_{10}$	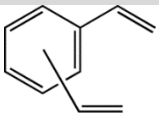	130.19	0.914	Alfa Aesar
Ethylene glycol dimethacrylate (EDGMA)	$C_{10}H_{14}O_4$	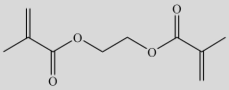	198.22	1.051	Sigma-Aldrich
Hydroxytyrosol	$C_8H_{10}O_3$	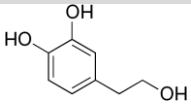	154.16	--	Merk
Methacrylic acid (MAA)	$C_4H_6O_2$	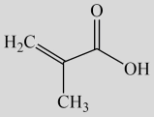	86.60	1.02	Sigma-Aldrich
Methanol (MeOH)	CH_3OH	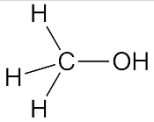	32.04	0.792	Fisher Chemical
N,N'-Methylenebisacrylamide (MBAm)	$C_7H_{10}N_2O_2$	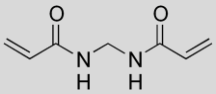	154.17	--	Sigma-Aldrich
N-propyl-N-(2,3-dihydroxypropyl) perfluoro-n-octylsulfonamide CAS: 2262-49-9	$C_{14}H_{14}F_{17}NO_4S$	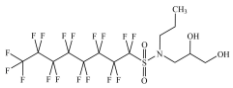	615.30	--	BIOSYNTH Carbosynth
Oleuropein	$C_{25}H_{32}O_{13}$	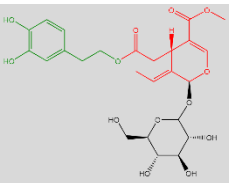	540.52	--	PanReac

Table 1: Continuation of the reagents used during synthesis and material evaluation.

Perfluorocyclohexane (PMC)	C_6F_{12}	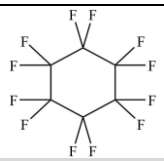	300.05	1.684	Sigma-Aldrich
Quercetin	$C_{15}H_{10}O_7$	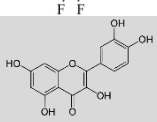	302.24	--	Acros Organics
Rutin	$C_{27}H_{30}O_{16}$	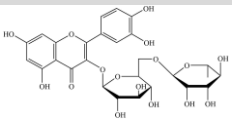	610.52	--	Acros Organics
Styrene (STY)	$C_6H_5CHCH_2$	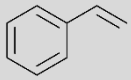	104.15	0.909	Acros organics
Tyrosol	$C_8H_{10}O_2$	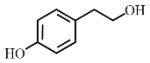	138.16	--	Merk
Vanillic acid	$C_8H_8O_4$	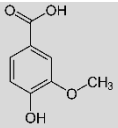	168.14	--	Sigma-Aldrich
Vanillin	$C_8H_8O_3$	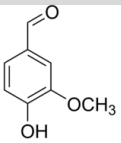	152.15	1.06	Sigma-Aldrich
Tetramethoxysilane (TMOS)	$C_4H_{12}O_4Si$	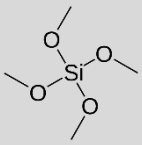	152.22	--	Thermoscientific
Verbascoside	$C_{29}H_{36}O_{15}$	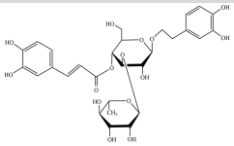	624.59	--	Merk

4.2. Equipment

The equipment used in this study are described in *Table 2*.

Table 2: Description of the equipment used throughout this work.

Equipments	Model	Brand
Analytical balance	AS/220/C/2	RADWAG
Orbital shaker	SSMI	Stuart
Vacuum pump	RE30022C	Stuart
Laboratory centrifuge	Scanspeed mini	LABOGENE
	Centrifuge 5810 R	Eppendorf
	CompactStar CS 4	VWR
Heating plate	VMS-C7	VWR ADVANCED
pH meter	inoLab	WTW
SPE system	Manifold Standard 12 – Port Model	SIGMA ALDRICH
Stirring plate	S03 series	Lbx instruments
UV reactor	--	Paralab
Vacuum Oven	22	Vacuell
Ultrasound	ULTRASONS-H	P SELECTA
	SW 1	SONO SWISS

4.2.1. UV-Vis Spectrophotometer

UV-Vis spectroscopy is one of the most simplified and economical techniques for examining analytes, this is a type of absorption spectroscopy in which UV-visible light is absorbed by the molecule. The one used for this work is the P9 Double Beam UV-Visible Spectrophotometer from VWR® as shown in *Figure 12.*

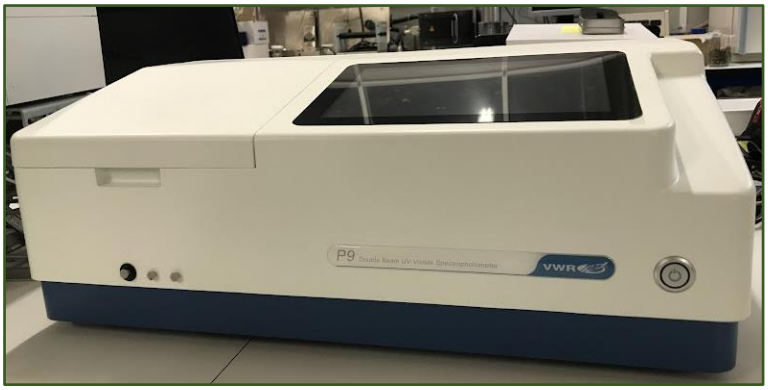

Figure 12: UV-Visible equipment used during this work.

4.2.2. High-performance liquid chromatography (HPLC-DAD)

High-performance liquid chromatography (HPLC-DAD) is a separation technique that can be very sensitive, specific, and precise. It is a particular form of column chromatography used to separate, identify, and quantify the active compounds in a mixture. When performing an analyse, variables such as the type of column, the solvent, and the gradient (since in HPLC-DAD there is two mobile phases) should be considered.

CHAPTER 5. RESULTS AND DISCUSSION

As it is known, obtaining extracts from plant matrices is greatly influenced by the combination of parameters such as extraction technique, extraction time, and, mainly, the solvent used.

5.1. Adopted extraction technique

Based on previous studies by this research group, ultrasound-assisted extraction (ultrasound-assisted digestion) and supercritical CO_2 extraction were the extraction methods of choice.

5.1.1. Ultrasound assisted (USA) digestion of olive leaves

Different varieties of olive leaves had been dried at room temperature (coded as A) and at 100°C for 2 hours (coded as B). The dried leaves were milled, 5 g of each variety was weighed into a 100 mL glass flask. Immediately after the addition of 50 mL of the solvent ethyl acetate, ethanol/water 80:20 and ethanol water 50:50. The digestion of the leaves was conducted for 1 h at 40ºC ±2ºC under ultrasonic irradiation. Captured images recorded those steps and are below displayed as *Figure 13.*

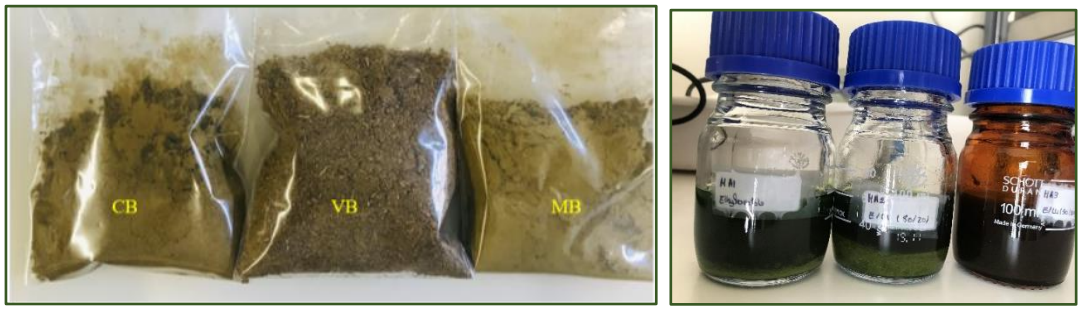

(1) (2) (3) (4)

Figure 13: Photographic record of the ultrasonic extractions performed with olive leaves using three solvents: (1) Crushed dried leaves. (2) Extract obtained with ethyl acetate. (3) Extract obtained with ethanol/water (80:20). (4) Extract obtained with ethanol/water (50:50).

The filtered liquid extract was evaporated in the rotavapor contemplating a distilled water bath at 40ºC. The samples extracted with ethyl acetate were dried in the oven at 45ºC and the remaining were freeze-dried, giving rise to a dry extract, detailed data on the conditions and results of the experiment are shown in *Table 3*.

Table 3: USA digestion of olive leaves with different solvents.

Sample ID	Leaves Variety	Solvents (50 mL)	Sample mass (g)	Extraction yield (%)
MA1	Madural A	Ethyl Acetate	5.01	11.35
MA2		Ethanol/water 80:20	5.02	29.98
MA3		Ethanol/ water 50:50	5.02	25.61
MB1	Madural B	Ethyl Acetate	5.01	7.70
MB2		Ethanol/ water 80:20	5.01	27.69
MB3		Ethanol/ water 50:50	5.00	28.61
VA1	Verdeal A	Ethyl Acetate	5.01	10.46
VA2		Ethanol/ water 80:20	5.00	29.54
VA3		Ethanol/ water 50:50	5.01	28.71
VB1	Verdeal B	Ethyl Acetate	5.01	7.41
VB2		Ethanol/ water 80:20	5.01	23.74
VB3		Ethanol/ water 50:50	5.01	23.99
CA1	Cobrançosa A	Ethyl Acetate	5.00	7.35
CA2		Ethanol/ water 80:20	5.00	22.09
CA3		Ethanol/ water 50:50	5.03	22.74
CB1	Cobrançosa B	Ethyl Acetate	5.06	6.87
CB2		Ethanol/ water 80:20	5.00	23.38
CB3		Ethanol/ water 50:50	5.06	25.19

* A: dried at room temperature. | B: dried at 100 ºC.

Afterwards, the solid extract was weight, the data allowed to obtain the extraction yield, and as expected, the extraction performs best with a mixture of ethanol and water. It was also possible to verify that increasing water percentage from 20 to 50 did not have substantial impact on the extraction yield.

The use of pure solvent (ethyl acetate) originated a substantial decrease on the extraction yield, this phenomenon agrees with results found in the literature [32]. Yateem, H. et al. (2014), reported the high performance of the mixture ethanol/water 80:20, in his analyses all pure solvents exhibited low yield.

It is worth mentioning that, although some studies indicate that methanol as a good solvent to extract oleuropein (a fact that justifies its use in methodologies to quantify the compound), it has a high toxicity and can compromise the use of extracts in foodstuffs [33].

In addition to the extracts present in *Table 3*, extracts whose oleuropein percentage is known were also used, this has enabled to broaden the purification/concentration pathways. These are detailed in *Table 4*.

Table 4: Specifications of the olive leaves extracts from NATAC Group.

Extract	Oleuropein percentage (%)
NATAC 20	20
NATAC 40	40
NATAC 70	70

5.1.2. Supercritical Extraction with CO_2

The supercritical CO_2 extraction system used includes basically the following components: a CO_2 source, a high-pressure pump (compressor), an extractor vessel, a decompression valve, and a separation chamber, it also has a few temperature and pressure controllers.

The pressurized CO_2, in liquid state, is supplied to the system through the compressor, going through a preheating, where the temperature is raised, thus occurring the passage from the liquid state to the supercritical state. The supercritical CO_2, as it flows through the system, passes through the solid vegetable matrix that is in the extraction chamber.

The exiting CO_2 undergoes depressurization, and when the pressure and temperature are reduced, the extract precipitates in the extractor. The software used assists in visualizing and recording the operating conditions, so there is adequate control of the experiment.

(1) (2) (3)

Figure 14: Photographic record of: (1) dry mass of olive lives inside the extraction chamber. (2): Recovery of the extract from the extractor. (3) Exhausted leaves.

Table 5: CO_2 Supercritical extraction of olive leaves with different solvents.

Extraction	Leaves Variety	Mass of dry leaves (g)	Solvent in the reactor	Volume of solvent in the reactor (ml)	Solvent in the trap	Volume of solvent in the trap (ml)
1	Cobrançosa	100	Ethanol	100	Ethanol	50
2	Verdeal	100	Ethyl Acetate	100	Ethyl Acetate	50
3	Madural	100	--	--	Ethanol	100
4	Verdeal	100	--	--	n-hexane	100
5	Cobrançosa	100	--	--	DI water	125

Supercritical fluid extraction (SFE) offers a fast and selective extraction method that besides using small volumes of organic solvents results in concentrated extracts. The supercritical extraction was implemented in this work for the extraction of bioactive from olive leaf by varying the solvent used, as described in *Table 5*. Each extraction lasted 2h with conditions of pressure and temperature around 150 bar and 40ºC, respectively.

5.1.3. HPLC-DAD analysis of olive leaf extracts

The HPLC-DAD analysis of the different analytes was performed using a linear gradient starting with 100% of solvent A (water/acetonitrile 90:10) and ending with 100% of solvent B (water/acetonitrile 10:90) for 45 minutes at 45ºC at a flow rate of 1mL/min. Both solvents were adjusted to a pH of 3 using acetic acid. The reverse phase column used was an Ascentis-C18, 5µm (25cm×4.6 mm) from Agilent USA.

Figure 15: HPLC-DAD used for the analysis.

Figure 16: C18 column used for the analysis.

The fingerprints were recorded at optimized wavelengths of 230, 250, 255 and 280 nm. The solvent solutions were vacuum degassed with vacuum pump prior to usage and all samples and standards were filtered quickly through a 0.2 µm membrane filter. The degradation products were identified by comparison with both the retention times and spectrum of all standard compounds. Quantification was possible by the use of calibration curves prepared from the HPLC-DAD peak areas of each standard.

After injection of a selection of extracts (MA1, MA2 and MA3) in HPLC-DAD, following the gradient previously described, it is evident that the extracts obtained with aqueous mixtures are much more complex than those obtained with ethyl acetate, as seen in *Graphic 1*. The HPLC-DAD analyses for the other extracts used in this work can be found in *Appendix A.*

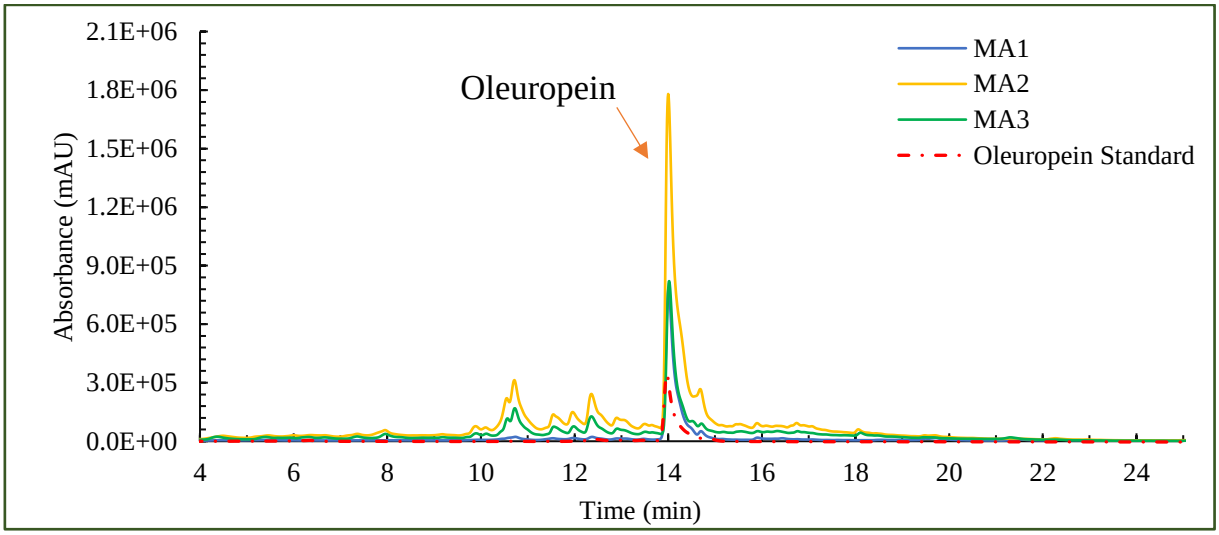

Graphic 1: HPLC-DAD analysis of olive leaf extract MA1 (in acetonitrile). MA2 (in ethanol/water 80:20). MA3 (in ethanol/water 50:50). Compared to oleuropein standard (in ethanol/water 90:10). λ=280 nm.

Table 3 shows values for yield expressed as mass of sample/dry mass of extract (global yield) and seen from this perspective the best solvent for extraction is a mixture of ethanol/water, however, analysing *Graphic 1* it can be seen that if the oleuropein content for each extract is determined, the conclusion of the most suitable solvent is ethyl acetate.

Although ACN is often cited as a solvent in this type of extractions, it is not considered a green solvent, this is one of the reasons why in this work besides ethanol/water, ethyl acetate is used. Ethyl acetate has been reported to perform well in oleuropein extraction and is ranked the highest among the tested solvents in the GSK solvent recommendation list [34].

5.1.3.1. Standards analysed in this work

Figure 17 shows a few of HPLC-DAD analysis for the polyphenol standards used in this work in the context of the identification of families of compounds present in the olive leaves extracts. The chromatograms of the standards presented in the referred figures, and those attached in *Appendix B*, made it possible to assess the elution region

of some polyphenols contained in the extracts. In parallel, the respective UV-VIS absorption spectrum of these standards was used as supplementary information to adjunct the identification of these molecules in the complex mixtures that constitute the real extracts of olive leaves.

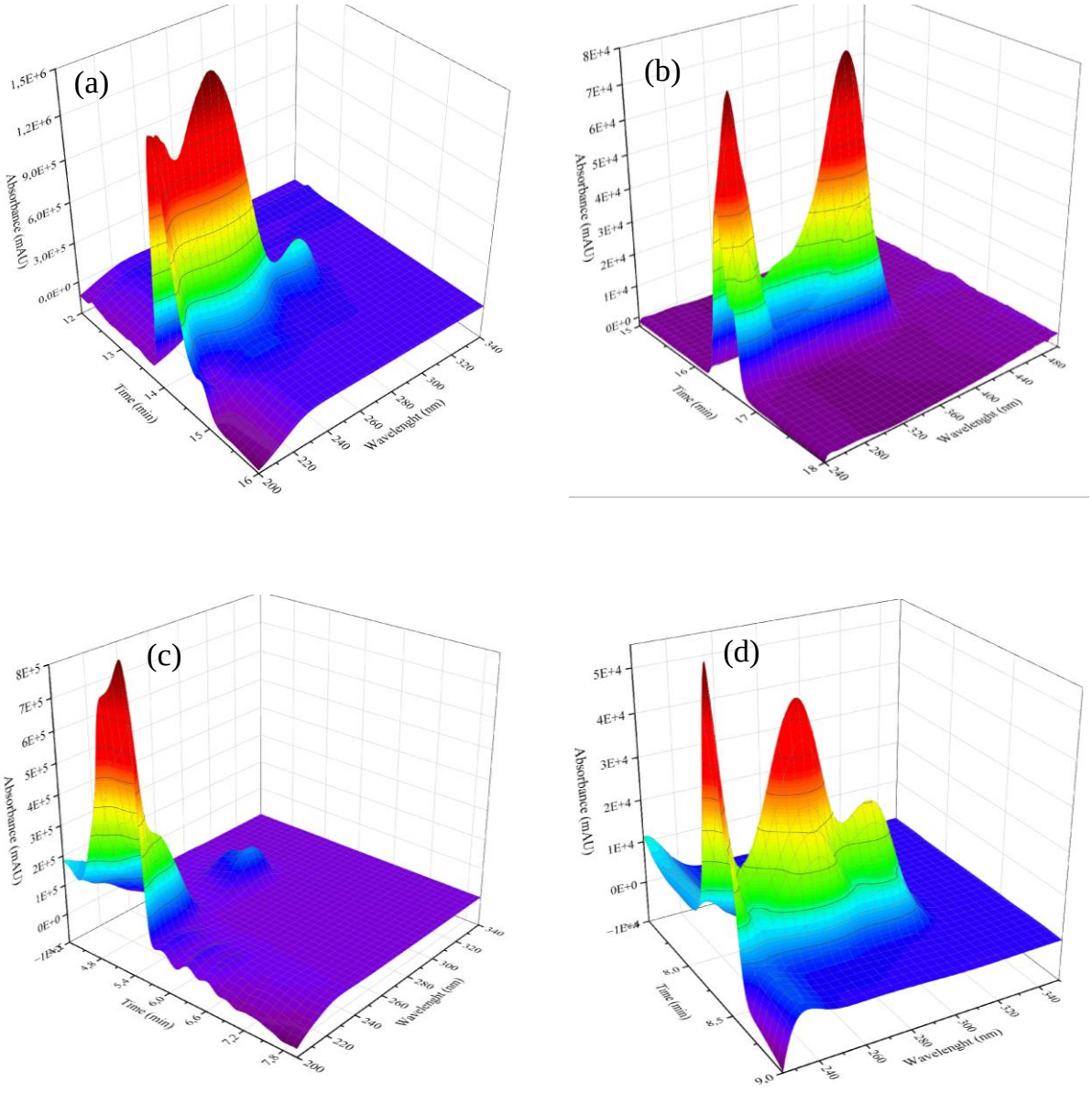

Figure 17: HPLC-DAD analysis of the standards for comparison with the phenolic profile observed in olive leaf extracts. (a): Oleuropein. (b): Quercetin. (c): Hydroxytyrosol. (d): Vanillic acid.

5.2. Synthesis of Molecularly Imprinted Polymers (MIPs)

For the synthesis of molecularly imprinted materials, the non-covalent approach was considered using FRP by precipitation (with both thermal and photo initiation being considered), by condensation and, by suspension. *Tables 6-9* refers to the synthesis conditions of the different MIPs and their analogue NIP.

In the synthesis of MIPs, oleuropein was used as the main template molecule, however other molecules, such as vanillic acid, tyrosol, and quercetin has also been considered. The use of templates belonging to different families comes from the perspective of including points of interaction common to the polyphenols potentially present in the extracts. Some of the used template molecules present considerable similarities at structural level with some polyphenols present in olive leaves, so it is admitted the creation of cavities with some specificity in the produced adsorbents.

Table 6: Conditions used to produce the molecularly imprinted adsorbents developed in this research. Synthetic MIPs.

MIP	Template	Functional Monomer 1	Functional Monomer 2	Functional Monomer 3	Crosslinker	Solvent	Initiator	YM (% massic)	YI (% molar)	YCL (% molar)	YFM/T (molar)	YCP/MP	Type of Initiation
MIP1	Oleuropein	4VAN-BTPI	Styrene		EGDMA	ACN (100)	AIBN	22.9	1.8	83.3	3		Thermal (60ºC)
MIP2	Oleuropein 70%	4VP	Styrene		EGDMA	ACN (100)	AIBN	20.4	1.8	83.3	3		Thermal (60ºC)
MIP3	Oleuropein 70%	4VP	Styrene	Acrylamide	EGDMA	ACN (100)	AIBN	20.4	1.7	75	3		Thermal (60ºC)
MIP6	Oleuropein 70%	4VP	Styrene		EGDMA	MeOH (100)	VA044	17.9	2	83.4	3		Thermal (40ºC)
MIP7	Oleuropein 70%	4VP	Styrene		MBAm	MeOH (100)	VA045	8.5	2	87.5	3		Thermal (40ºC)
MIP8	Oleuropein	AAm			EGDMA	ACN (100)	AIBN	23.8	3.1	93.9	7.7		Photo
MIP9	Oleuropein	AAm			EGDMA	ACN (100)	AIBN	23.8	3.1	93.9	15.7		Photo
MIP10	Oleuropein	AAm			EGDMA	ACN (100)	AIBN	23.8	2.4	60.5	9.9		Photo
MIP11	Oleuropein	AAm			EGDMA	ACN (100)	AIBN	29.4	2.1	68.2	65.6		Photo
MIP12	Oleuropein	AAm			EGDMA	ACN (100)	AIBN	29.4	2.1	68.3	65.7	0.01	Photo / Suspension
MIP15	Vanillic Acid	4VP	MAA	Acrylamide	EGDMA	ACN/DMSO (98/2)	AIBN	27.9	1.8	70	3		Photo
MIP16	Vanillin	4VP	MAA	Acrylamide	EGDMA	ACN/DMSO (98/2)	AIBN	27.9	1.8	70	3		Photo
MIP17	Tyrosol	4VP	MAA	Acrylamide	EGDMA	ACN/DMSO (98/2)	AIBN	27.9	3.5	69.8	3.7		Photo
MIP18	Verbascoside	4VP	MAA	Acrylamide	EGDMA	ACN/DMSO (98/2)	AIBN	27.9	4.2	69.8	54.3		Photo
MIP19	Caffeic Acid	4VP	MAA	Acrylamide	EGDMA	ACN/DMSO (98/2)	AIBN	27.9	3.6	69.9	3		Photo
MIP20	Rutin	4VP	Styrene		EGDMA	ACN/DMF (85/15)	AIBN	12.8	2.1	40	43		Thermal (60ºC)
MIP21	Quercetin	4VP	Styrene		EGDMA	ACN/DMF (85/15)	AIBN	5.9	4.7	40.1	3		Thermal (60ºC)

Table 7: Conditions used to produce the molecularly imprinted adsorbents developed in this research. Synthetic - Synthetic MIPs.

Material	Core	Template	Functional Monomer	Crosslinker	Crosslinker 2	Initiator	Solvent	YM (% massic)	YI (% molar)	YCL1 (% molar)	YCL2 (%molar)	YFM/T (molar)	Y core (% mass)
MIP4	P4VP*	Oleuropein	MAA	EGDMA	DVB	AIBN	ACN	4.5	5.8	16.7	66.7	4.3	1.8

Table 8: Conditions used to produce the molecularly imprinted adsorbents developed in this research. Natural - Synthetic MIPs.

Material	Core	Template	Functional Monomer 1	Functional Monomer 2	Functional Monomer 3	Crosslinker 1	Initiator	Solvent	Ligand	Catalyst	YM (% massic)	Y M/Br (molar)	Y Cu/Br (molar)	Y L/I (molar)	YCL (% molar)	YFM1/T (molar)	YFM2/T (molar)	YFM3/T (molar)
MIP5	MCC-Br	Oleuropein	4VP	Styrene	Aam	EGDMA	MCC-Br	DMSO	PMDETA	CuBr	13.16	12.3	0.98	1	75.8	2.0	1	3.77e-3

Table 9: Conditions used to produce the molecularly imprinted adsorbents developed in this research by condensation.

	Molar Ratios					
	TMOS	Ethanol	Water (pH 13) NaOH (0,01M)	Oleuropein	3-(Aminopropyl)trimethoxysilane	1-[3-(Trimethoxysilyl)propyl]urea
MIP13	1	20	7	0.003	0.01	
MIP14	1	20	7	0.003		0.01

The composition of the polymerization system (defined by the parameters YM, YI, YCL, YFM/T and YC/D) follows the principles of molecular imprinting and is based on previous results of this research group with polyphenols. These parameters are defined as:

- YM: refers to the mass fraction of functional monomer + crosslinker in the polymerization solution (%).
- YI: refers to the mole fraction of initiator relative to functional monomer + crosslinker (%).
- YCL: refers to the molar fraction of crosslinker in the functional monomer + crosslinker mixture (%).
- YFM/T: refers to the molar ratio between functional monomer and template molecule.
- YC/D: refers to the mass ratio between the oil phase and the monomer phase in reverse suspension polymerization.

The morphology of the MIPs was changed mainly by the specification of the parameter YM. If this parameter assumes values below 10% it generally gives rise to individual microparticles, bulky materials (needing posterior grinding) results from higher YM fractions [35]. Apart from the type/amount of monomer used and the type of solvent, the presence/absence of template also influences the size of particles formed. For instance, in the case of MIP4, its analogue NIP4 had to be withdrawn from testing as under certain conditions the particles passed through the fritz. Using SEM (Scanning electron microscope) analysis, the impact of the synthesis conditions on the morphology of other MIPs synthesised by this group has been analysed and can be seen in [35-37].

The influence of the template in particles morphology can be visually observed in *Figures 18 and 19*, where it is compared two different templates (Rutin and Quercetin). As can be observed in *Table 6*, MIP20 and MIP21 were synthesized following similar criteria (same solvent ratio, same monomers, and initiator), however, these materials present distinct morphologies, the particles of MIP21 are considerably

smaller than those of MIP20, fruit of a YM/T more than 10x smaller. This demonstrates that the template can also be used to manipulate the particle size.

Figure 18: Photographic record of the MIP synthesized considering rutin as template. MIP20.

Figure 19: Photographic record of the MIP synthesized considering quercetin as template. MIP21.

5.2.1. Synthesis of Molecularly Imprinted Polymers by Precipitation

The setup used to perform this synthesis consisted of a paraffin bath with constant temperature control, as shown in *Figure 20.* After solubilizing all the components on the solvent, the resulting solution is carefully purged using argon gas in order to prevent inhibition. This solution is then submerged into the bath under stirring between 24 and 48 hours.

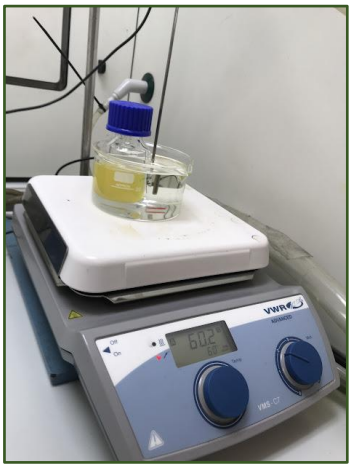

Figure 20: Photographic record of the synthesis with quercetin at 60ºC. MIP21.

Figure 21: MIP21 after 48h under reactional conditions.

.

5.2.2. Synthesis of Molecularly Imprinted Polymers by suspension

To prosecute this type of synthesis, a photo reactor was used, the reactor itself is made of quartz, and it is composed of a paddle agitator. This reactor is placed inside a mirrored chamber with four 7.1 W UV lamps from Philips as shown in *Figure 22-(1)*.

For this synthesis, it was necessary to dissolve all the MIP making reagents on the discontinuous phase, while the surfactant used (N-Propyl-N-(2,3-dihydroxypropyl)perfluoro-n-octylsulfonamide CAS: 2262-49-9) is to be in the continuous phase (PMC) .

(1) (2) (3) (4)

Figure 22: (1) – Power Lamps inside reactional chamber. (2) – Solubilized reagents to synthesize MIP12, immiscible phases under degassing. (3) – Testing of agitation speed. (4) – MIP12 after 6h of reaction.

Once the mixtures for the continuous and discontinuous phases were prepared, they were put in contact inside the reactor, as shown in *Figure 22-(2).* The degassing process was carried out from the bottom of the reactor, after which the paddles were switched on, the chamber was carefully closed, and the reaction was started by switching on the UV lamps. At the end of 6 h the reaction was interrupted.

Due to the type of paddles/agitation used, the occurrence of the formation of spherical and bulk particles was verified, the vortex formed pushed the particles against the wall of the reactor, which aggregated and formed a film on the walls of the reactor. *Figures 23 and 24* show the particles obtained with random sizes and geometry and with homogeneous average size respectively.

Figure 23: Results for MIP12 suspension, particles of random size and geometry.

Figure 24: Results for MIP12 suspension, particles with average hemogenic size

5.2.3. Fourier transform infrared spectroscopy (FT-IR)

In this work, FT-IR analysis was performed for the imprinted materials to determine the presence of functional groups and bond types, it is known from previous works of this group [35,38] and from the literature that in a successful polymerization MIP and NIP present a similar chemical spectrum.

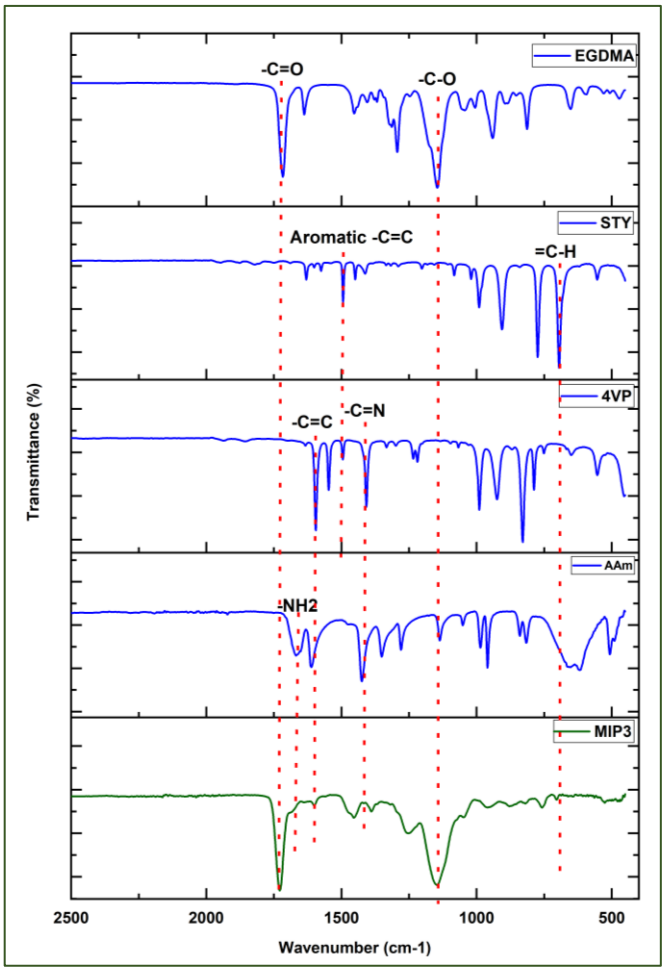

Figure 25: FTIR spectra of MIP3 and its corresponding monomers (4VP, AAm, STY) and crosslinker (EGDMA).

The FT-IR spectrum of MIP3, *Figure 25*, clearly show the incorporation of the crosslinker (EGDMA/ C=O at 1716 cm^{-1} corresponding to the ester group) in the final polymeric network. The incorporation of monomers in the final product is also demonstrated with the presence of small bands of the vinyl groups (-C=N 1407 cm^{-1}) from 4-vinylpiridine, the typical aromantic ring =C-H (at 706 cm-1) from styrene, and amine group $-NH_2$ (1673 cm^{-1}) from Acrylamide.

In regard to the monomers, FT-IR spectra for MIPs produced with different FM but using a high amount of EGDMA crosslinker (>70%) shows that with these systems, the IR assignments associated with EGDMA prevails in the spectra showing a lower specific functionalization of the materials. The same behaviour is observed with others synthetised materials attached in *Appendix C.*

5.3. Material regeneration after synthesis

After synthesis, the template removal process is crucial for successful assessment of the MIPs. During this work two methods was considered as regeneration steps.

5.3.1. Centrifuge

The synthetized material was carefully transferred to a 15 mL falcon tube and the solvent methanol/acetic acid 90:10 was added until maximum capacity of the tube. The tubes were then centrifuged for 8 minutes at 6500 RPM. At the end of this time, the tubes were left to rest, part of the solvent was removed, taking care not to lose mass, and the solvent was added up to 13 mL. Washing steps with methanol/acetic acid 90/10, methanol, and ethyl acetate were followed by UV-VIS spectrum readings to check the washing performance. Thereafter, the materials were taken to the oven at 45ºC and 0.3 bar for 72 hours.

Figure 26: Photographic record of regeneration by centrifugation.

Figure 27: Photographic record of MIP7 after centrifugation.

.

5.3.2. Dialysis

The polymerized material was carefully transferred to a SnakeSkin dialysis tubing (3.5 K MWCO from thermoscirntific) and placed into a beaker, filled with methanol/acetic acid 90:10. At each 24 h the solvent was replaced, following order: methanol/acetic acid 90:10, methanol. At the end, the SnakeSkin containing the material were taken to the oven at 60ºC for 48-72 hours.

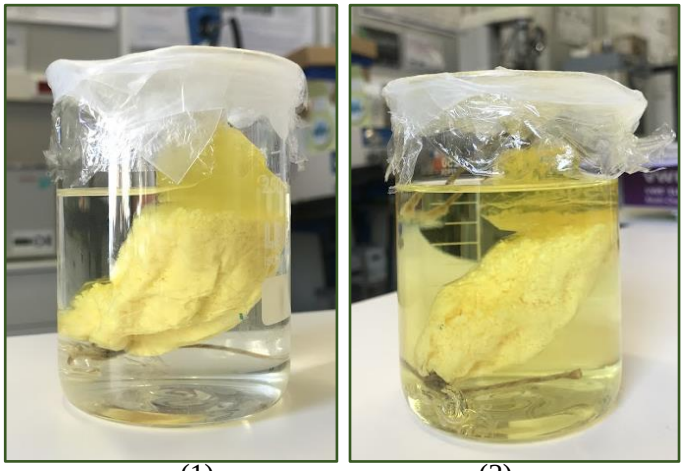

(1) (2)

Figure 28: Photographic record of the regeneration by dialysis of MIP20. (1) – Material in Methanol. (2) – Material after 24 hours in Methanol.

5.4. Solid phase extraction (SPE)

The SPE was carried out by weighting 100 mg of the MIP and the correspondent NIP into plastic syringe vials containing a 20 μm diameter fritz. In order to evaluate the retention performance, some commercial resins, namely XAD4, XAD7HP, REIILLEX402, REILLEX425, DAX8, and MICROCRYSTALLINE CELLULOSE (MCC) were also utilized under the same conditions. At first the solvent used during the extraction was added to the materials for their conditioning, once the solvent was removed, an extract or target molecule solution was loaded into the cartridge containing the aforesaid materials. At the outlet of each cartridge, the liquid phases were recuperated and their absorbances were measured by UV-VIS (at proper wavelength) and compared to the absorbance of the loading solution. This allows the determination of the retention and consequently to calculate the adsorption capacity of each material.

To further utilize the adsorbent materials, a step of regeneration is required which consists in washing the materials with methanol/acetic acid 90:10 (v/v) and with methanol, then conditioned with an appropriate solvent depending on the next solution to be used in the SPE (generally, the conditioning solvent is the same one as the solvent used during the loading). The solvent passed through the materials is then read on the UV-VIS (at proper wavelength) to check the performance of the washing of the materials.

Due to unsuitable morphology for continuous mode operation (e.g., presence of very small particles that pass through the fritz and thus increasing the UV-VIS response), some of the adsorbents described in *Tables 6-9* were not included in these experiments.

5.4.1. Retention and Selectivity tests

By the use of SPE it was possible to efficiently determine the retention capacity of the different synthesised materials, as shown in *Graphic 2* the molecule retention is strongly influenced by the solvent used.

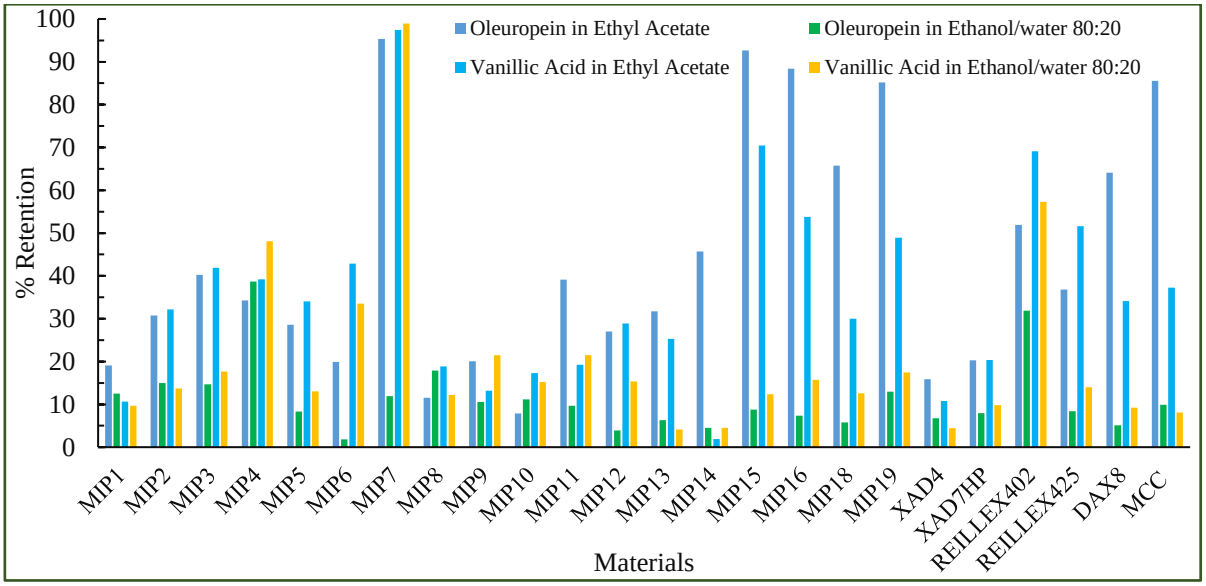

Graphic 2: SPE assessment of the various synthesized and commercial adsorbents, with oleuropein and vanillic acid solid in ethyl acetate and ethanol/water 80:20. Concentration equal to 0.28mM in all four scenarios.

When it comes to the oleuropein molecule, seen in *Graphic 2*, the preferential retention in the presence of ethyl acetate compared to ethanol/water 80:20 is remarkable. This is due to the possible competition of the second solvent to form hydrogen bonds with the materials, and to the greater affinity of oleuropein with more polar solvents as hydroalcoholic mixtures. Compared to vanillic acid (a metabolite of caffeic acid), although not so evident, the same behaviour is observed.

A parameter that influences the selectivity of MIPs is the size of the template, as has been reported, molecular imprinting with larger molecules generates less specific cavities, which results in less selective recognition of compounds of the same family. In a study performed by A. M.-Esteban et al., with the molecules isoproturon and fenuron, isoproturon-imprinted polymers were able to recognise all the herbicides studied whereas fenuron-imprinted polymers were highly selective [39]. Therefore, under the conditions tested, vanillic acid shows high retention in ethyl acetate.

With regard to the commercial resins, it is noted that there may be high retention, particularly with REILLEX402. In this way, as this research group have been demonstrating, the potentiality of the adsorbents synthesized with 4VP in the valorisation processes of bioactive present in vegetal matrices is reaffirmed.

It is worth mentioning that, generally, the commercial adsorbents used here, work reasonably well when they promote hydrophobic interactions, for example with nonpolar molecules (e.g., vanillic acid) present in aqueous media, in these cases, the molecule has a higher affinity with the adsorbent than with the solvent.

Compared to oleuropein, in ethanol/water 80:20, vanillic acid shows higher retention. Here, the relevance of the solvent is evident, as oleuropein is a polar molecule and vanillic acid is nonpolar, the latter will preferentially interact with the material in more polar media.

5.4.2. Loading, washing and elution tests

Still in SPE, loading, washing and elution tests were performed in order to reaffirm the results presented so far. In the loading step a solution of known concentration of oleuropein was used, in the washing step the same solvent in which the previous solution was made was used. A solvent with greater elution strength such as methanol/acetic acid 90:10 was utilized in the elution step. The three steps were performed with a volume of 2.5 mL, where, with the aid of the vacuum pump, the pressure was controlled so that the flow of the liquid phase would take about 7.5 minutes (≅ 0.33mL/mim). At the end of each of the three stages, the samples collected were duly identified and preserved for their subsequent analysis in UV-VIS.

The case shown in *Graphic 3* comes from the use of a real extract, (containing 70% oleuropein, NATAC 70) in ethyl acetate on materials chosen from the results of the previous tests (MIP3/NIP3, MIP7/NIP7, MIP11, MIP12 and REILLEX402).

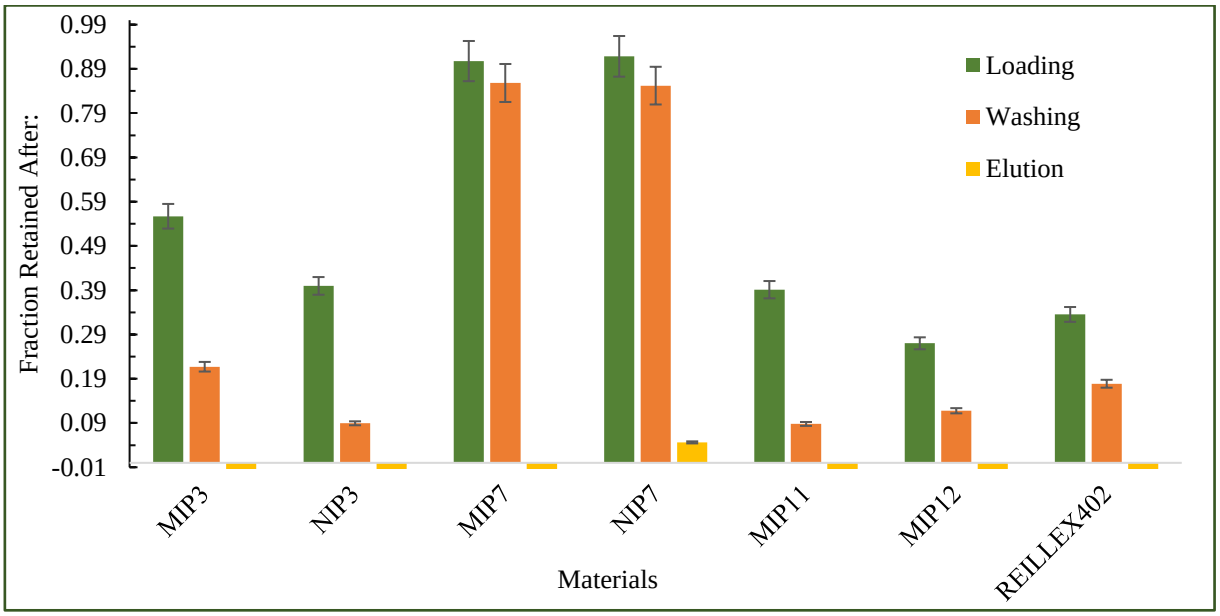

Graphic 3: Retention assessment in SPE of MIP3/NIP3, MIP7/NIP7, MIP11, MIP12 and REILLEX40. Loading with a 0.15mg/mL solution of NATAC 70 in ethyl acetate. Washing with ethyl acetate. Elution with methanol/acetic acid 90:10.

Analysing the results in *Graphic 3*, is possible to observe that MIP7/NIP7, in these conditions, presents a higher retention capacity in relation to other materials, even with commercial resin (REILLEX402). These good retentions capability can be justified by the use of a crosslinker that imparts high functionality to the material, MBAm, as it is considered a donor-receptor of electrons. Thereby, the effect of molecular imprinting can be masked by this functionality.

Comparing the assessment of MIP3 and REILLEX402, both synthetized with 4VP, the molecularly imprinting material seems to hold better retention capacity, as in the loading step MIP3 results excels those of REILLEX402. Compared to its non-imprinted analogue, NIP3, the amount retained in the loading step of NIP3 is lower than that of MIP3, this result serves as a proof of molecular imprinting of MIP3 and emphasizes the advantages of molecular imprinting over commercial resins in the purification/concentration of polyphenols.

With washing there is an expected reduction of retained amounts for all the presented adsorbents, as the name suggests, this step intends the removal of the compounds from the binding sites. Compounds that occupied the active binding sites by means of non-specific interactions are washed out of these cavities. Therefore, for MIP3 and NIP3 it can be said that oleuropein binds more specifically to the imprinted material (MIP3). Again, the effect of molecular imprinting is demonstrated, as even after washing, MIP shows higher retention than NIP.

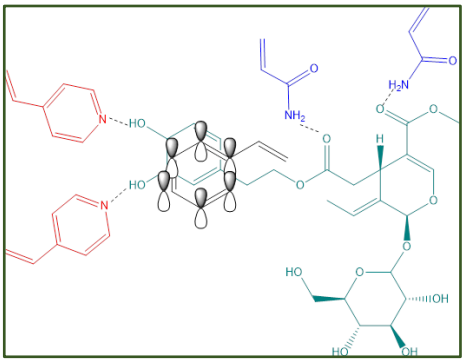

Figure 29: Expected interactions between monomers 4VP, STY and AAm with oleuropein in MIP3.

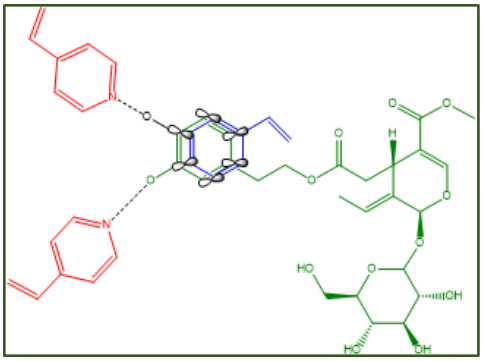

Figure 30: Expected interactions between monomers 4VP and STY with oleuropein in MIP7.

As displayed in *Table 6*, MIP11 and MIP12 differ in the type of polymerization, which confers to each different morphology. SPE testing with these materials revealed better performance of MIP11 (FRP by precipitation). This is justified due to the greater ease of adhesion to the imprinted sites that MIP11 offers, since it has smaller particles, for the same volume, there will be more imprinted sites available for adhesion of molecules, i.e., with particle size decrease, the adsorption rate constant increases.

In contrast, in the washing step one can readily see that the interactions of the polyphenols present in the extract is stronger with the material synthesized by suspension (MIP12), this result may be owing to the morphology of the particles. MIP12 may have active binding sites within its structure, and porosity, which hinders the exit of the molecules there retained.

The elution step requires the use of an appropriate solvent, with higher elution force, capable of breaking the analyte-adsorbent interaction and that is compatible with final analysis, so methanol/acetic acid 90:10 was used. It has been noted, for the cases presented in *Graphic 6* that the samples obtained suffer influence of the elution solvent, due to the different interaction of the molecule in the new solvent.

5.4.3. Saturation tests with MA1 extract

A material that exhibits high retention capacity, and selectivity, in theory would be ideal, as such a material is able to concentrate a given molecule, thus allowing fractionation of the extract. With these considerations in mind, a selection of materials (MIP3 and MIP7) was used in SPE for retention capacity testing. This study involved passing constant volumes of the olive leave extract, MA1, in ACN, until the UV response of the liquid phase obtained at the exit of the cartridge was equal/similar to the UV response of the loading solution. The outcome of these tests is presented in *Graphics 7 and 8.*

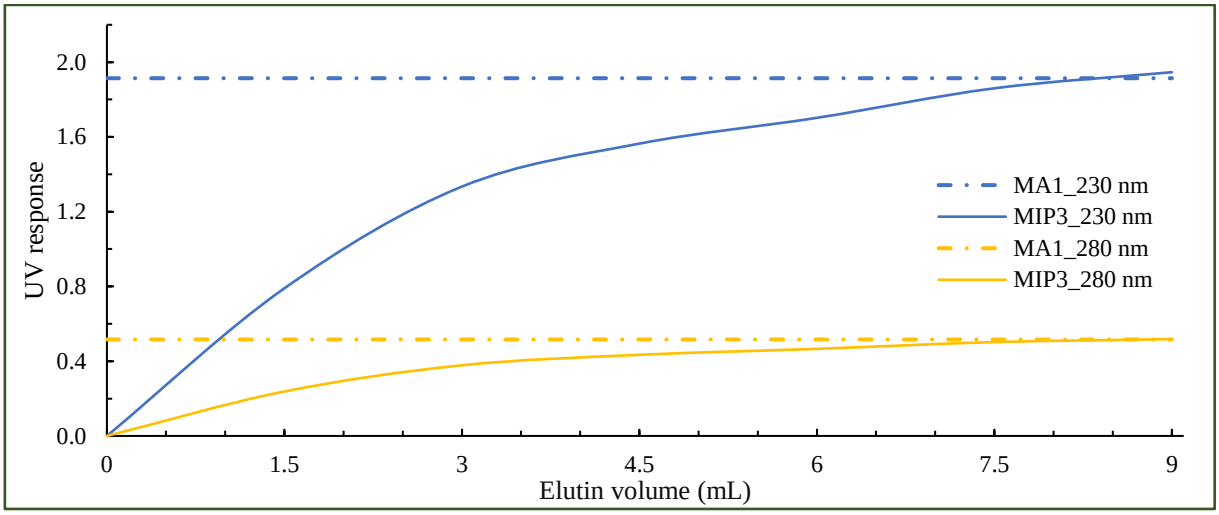

Graphic 4: Saturation profile of MIP3 with MA1 extract dissolved in ACN. Concentration equal to 0.2 mg/mL. λ=230 nm and 280 nm.

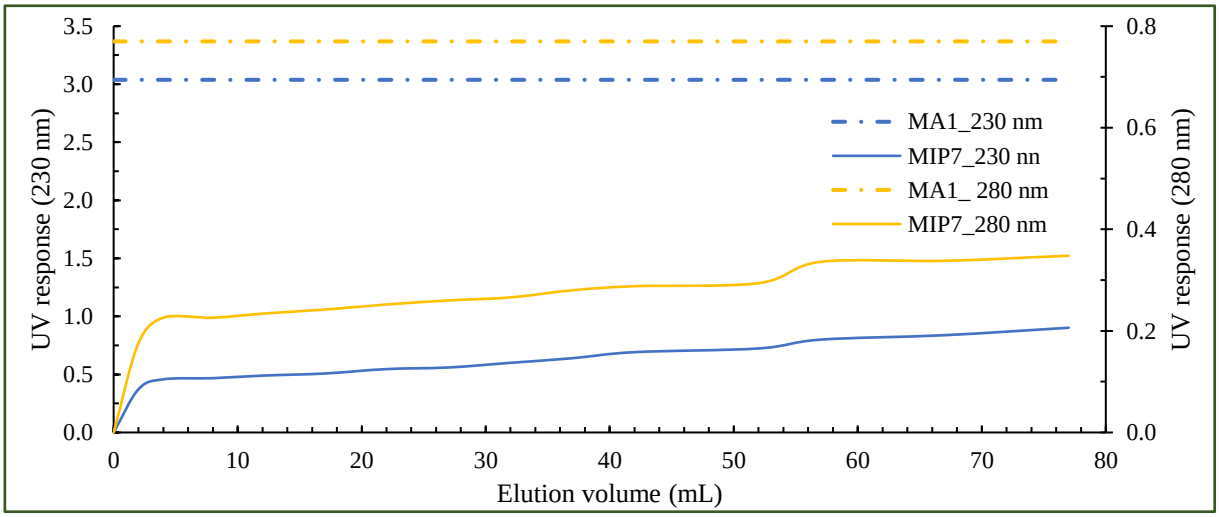

Graphic 5: Saturation profile of MIP7 with MA1 extract dissolved in ACN. Concentration equal to 0.2mg/mL. λ=230 nm and 280 nm.

The results obtained revealed that from the materials tested, MIP7 presents superior retention capacity, after passing 77 mL of solution it was still far from saturation. When tested in different solvent (ethanol/water 90:10) the distinction of MIP7 is also observed, as can be seen in *Appendix D, Graphics 22 and 23*, compared to REILLEX402 (98% of 4VP crosslinked with divinylbenzene), MIP7 holds about half the retention capacity of REILLEX402 under the stated conditions.

The retention capacity of MIIP7, relative to MIP6, observed in *Graphics 2,3 and 5* is due to the fact that the MBAm used in MIP7, as well as oleuropein, possess electron

donor and acceptor groups, thus more binding points are expected between oleuropein and MBAm than with EGDMA (used in MIP6).

HPLC-DAD analysis of some saturation fractions, *Graphic 6*, supported the results obtained for MIP7.

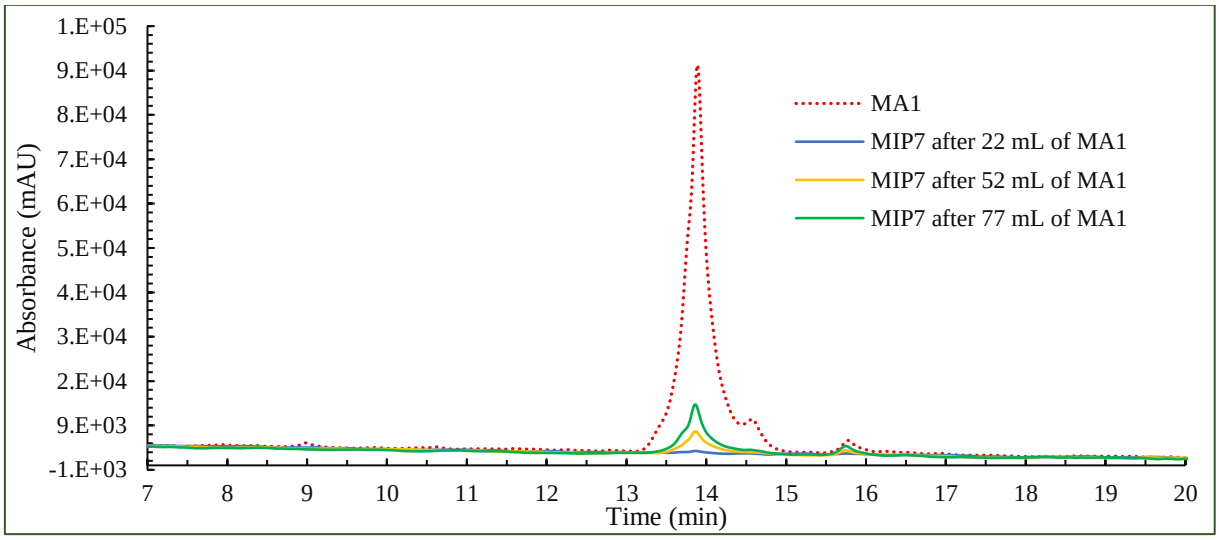

Graphic 6: HPLC-DAD analysis of MIP7 saturation profile with MA1 in acetonitrile with a concentration of 0.2mg/mL. λ=250nm.

Still in *Appendix D, Graphics 21 and 22*, it can be observed that the MIP7 presents a competitive retention profile, that is, the different adsorbates present in the extract compete among themselves for adsorption sites, in this way the adsorption of different substances such as polar and nonpolar compounds on the heterogeneous surface may occur on different types of sites.

The next step in the assessment of the MIP7 performance consisted in eluting the material with different solvents, starting from the one which presents the lowest elution power to the highest. Then, after passage of 77 mL of extract MA1, 3 mL of water, ACN, methanol and methanol/acetic acid 90:10 were passed consecutively, at room temperature. The results of which are shown in *Graphics 7 to 10.*

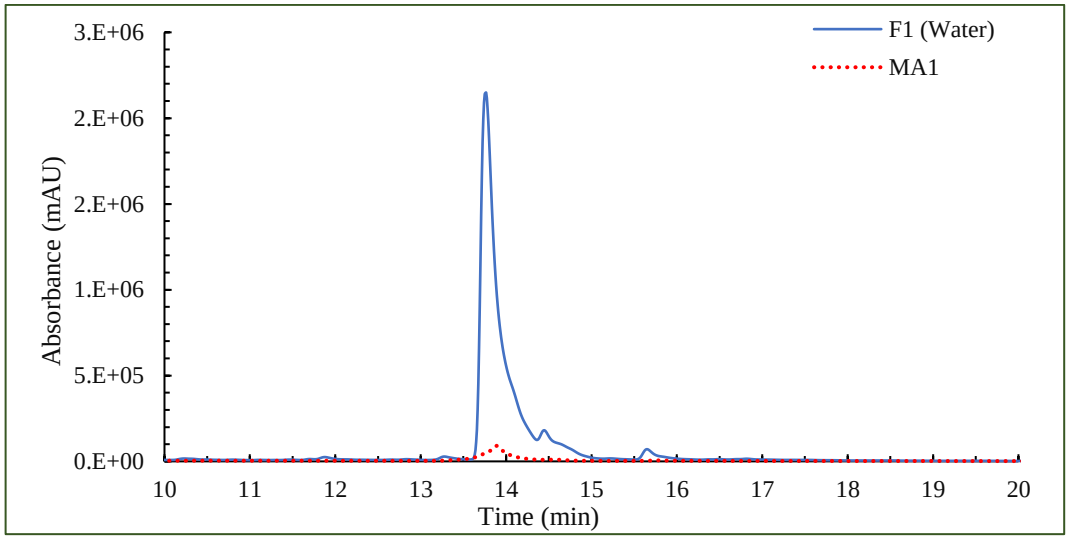

Graphic 7: HPLC-DAD analysis of the fraction eluted with water after saturation of the MIP7 adsorbent with the MA1 extract compared to the respective extract. λ=250 nm.

In the first fraction, *Graphic 7* there is a peak whose spectrum corresponds to that of oleuropein, and it is much more concentrated than the initial extract, elution with water allowed a concentration of oleuropein relative to other compounds present in the initial extract.

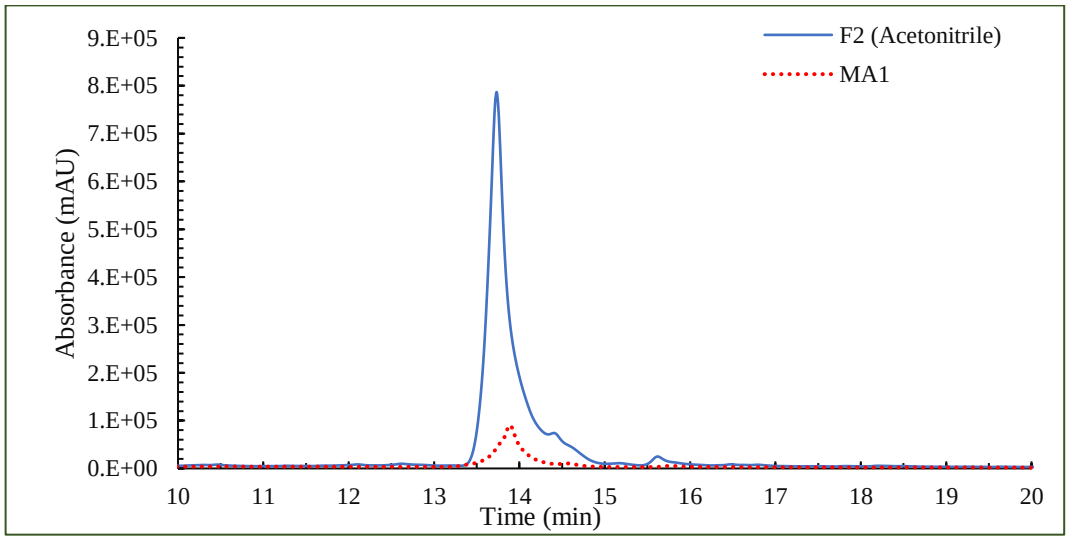

Graphic 8: HPLC-DAD analysis of the fraction eluted whit acetonitrile after saturation of the MIP7 adsorbent with the MA1 extract (0.2 mg/mL in ACN) compared to the respective extract. λ=250 nm.

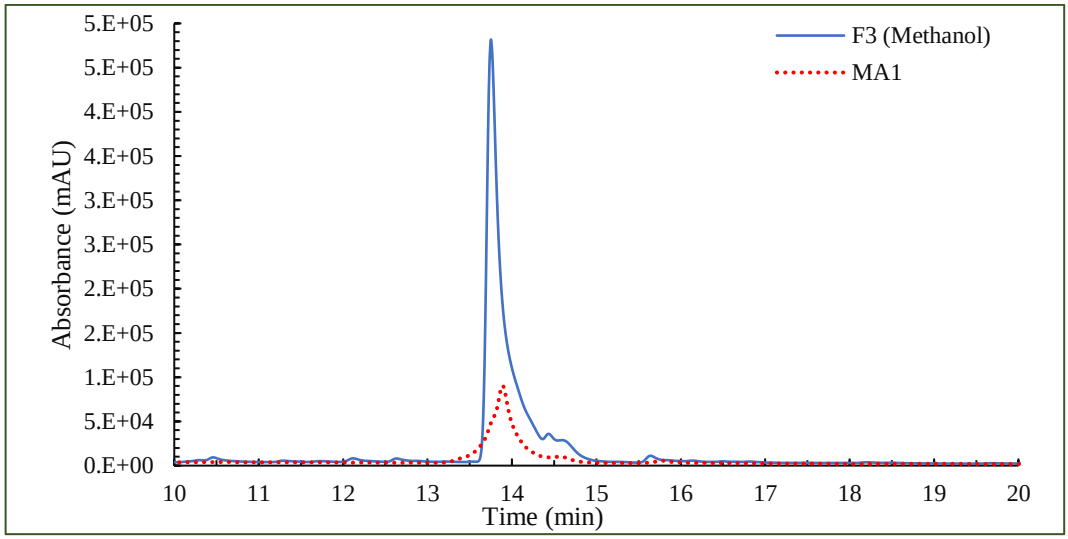

Graphic 9: HPLC-DAD analysis of the fraction eluted with methanol after saturation of the MIP7 adsorbent with the MA1 extract (0.2 mg/mL in ACN) compared to the respective extract. λ=250 nm.

The elution of the material with acetonitrile as well as with methanol, *Graphics 8 and 9*, also allowed purification and concentration of oleuropein in relation to the initial extract, a gradual oleuropein decrease is perceived with each elution.

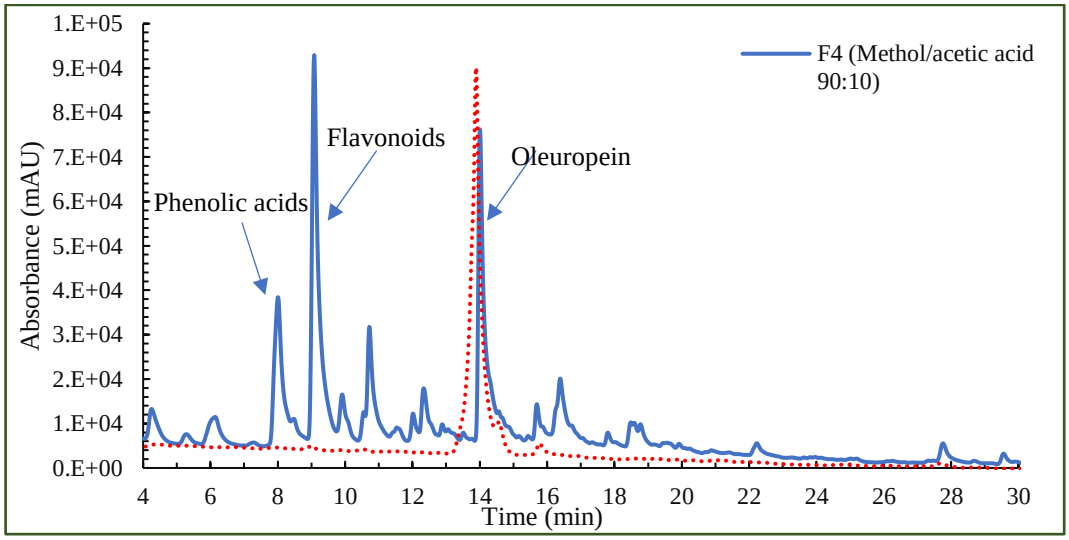

Graphic 10: HPLC-DAD analysis of the fraction eluted whit methanol/acetic acid 90:10 after saturation of the MIP7 adsorbent with the MA1 extract (0.2 mg/mL in ACN) compared to the respective extract. λ=250 nm.

In this last fraction, *Graphic 10*, the oleuropein peak appears in lower concentration in relation to the previous fractions and also to the extract. Compounds present in the initial extract whose elution times are inferior to those of oleuropein

appear more evident in this fraction. It is worth highlighting that the extract used, under the conditions presented, is by itself a rather simplified extract. However, these results, *Graphics 7 to 10*, corroborate the high retention of this material, and present its potential in the fractionation of real extracts.

5.5. Use of Chromatographic columns in continuous processes

This section will explore the use of MIP particles as adsorbents for continuous processes that can be elaborated for the retention and release of phenolic compounds. In this regard, the analysis includes the packing of MIP particles in chromatographic columns and the assessment of the possibility of the stable running of a continuous adsorption/desorption process.

A selection of material was chosen (MIP3, MIP7, MIP12 and REILLEX402) and with the aid of a vacuum pump, a predefined dry mass of these particles was packed into columns as presented in *Figure 32*. Each column has at both ends a system of multiple filters that prevents possible loss of mass (particles) during the process. *Table 10* describes the columns dimensions as well as the amount of material packed in each column.

Figure 31: Chromatography columns used in this work.

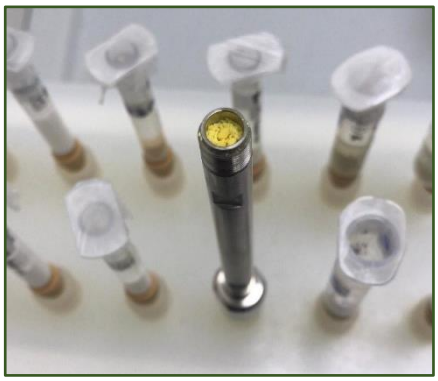

Figure 32: Photographic record of the packing process of MIP21 into chromatography columns.

:

Table 10: Packing specifications of materials in adsorption columns.

Material	Column length (mm)	Column intern diameter (mm)	Dry mass (mg)
MIP3	10	4.6	32.5
MIP7	50	4.7	159.3
MIP12	50	4.6	167.1
REILLEX402	30	4.6	1780

Once packed, the saturation process was carried out with a pump (KNUER P 4.1S) under the conditions described in *Table 11*.

Table 11: Specifications of the saturation procedure for the adsorbents MIP3, MIP7 and Reillex402 in column with Ethanol/water 90:10.

Material	Extract used	Solvent	Concentration (mg/mL)	Flow (mL/min)	Elution Volume (mL)
MIP3	NATAC 20	Ethanol/water 90:10	0.25	0.5	12.5
MIP7	NATAC 70	Ethanol/water 90:10	0.11	2	≅ 52
REILLEX402	NATAC 20	Ethanol/water 90:10	0.25	3	2070

At the end of the saturation process of MIP3 and REILLEX402, the initial solution and some samples collected during the saturation were analysed through HPLC-DAD. The results presented up to this point gave an anticipation of the retention capacity of the materials used in the column, and as seen in *Table 11*, REILEEX402 shows the highest elution volume. Turning to the HPLC-DAD analysis, it can be seen in *Graphics 11 and 12* the gradual retention of the phenolic compounds contained in the initial extracts.

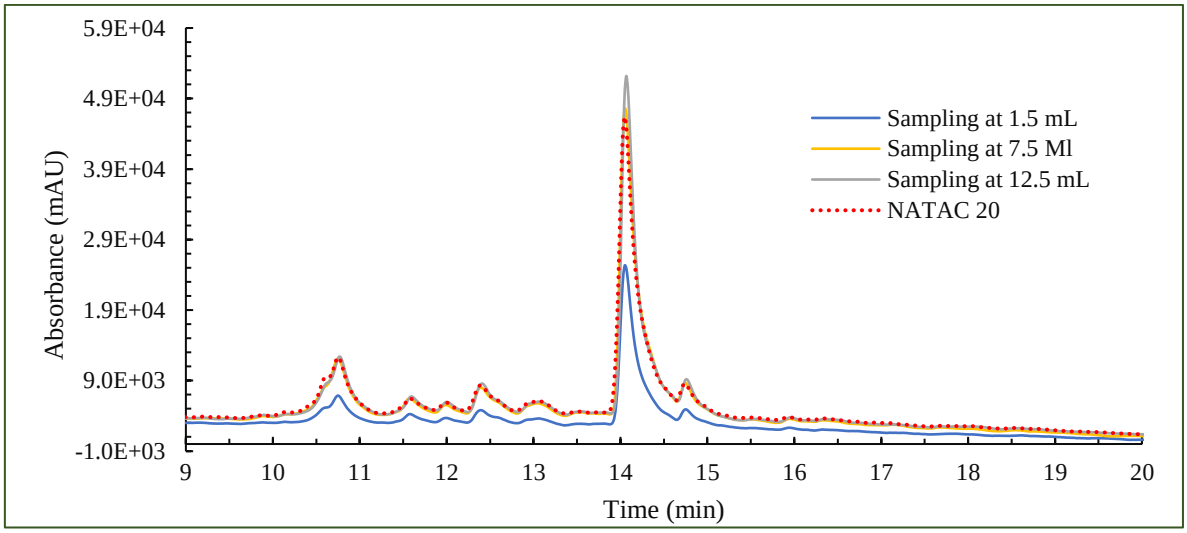

Graphic 11: HPLC-DAD analysis of NATAC 20 extract in comparison to the sampling in MIP3 after 1.5, 7.5, and 12.5 mL. λ=280 nm.

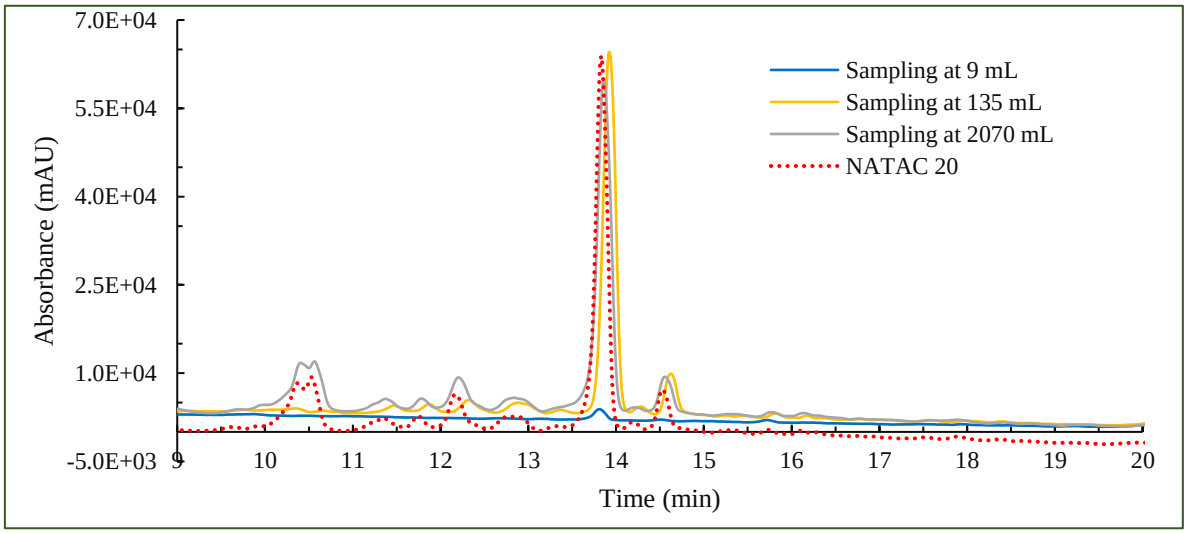

Graphic 12: HPLC-DAD analysis of NATAC 20 extract in comparison to the sampling in REILLEX402 after 9, 135, and 2070 mL. λ=280 nm.

In addition to the HPLC-DAD analysis, it is also possible to observe the material saturation process by means of the breakthrough curves. The information from a breakthrough curve, namely the retention capacity of the adsorbent for a given solute under specific operating conditions, is crucial for designing an efficient continuous process for the valorisation of polyphenols present in plant extracts. In this regard, *Graphic 13* presents the normalized breakthrough curve for the saturation in column of

MIP7. Where, the retained amount measured for the presented study was 10.28 µmol/g under the stated conditions, *Table 11*.

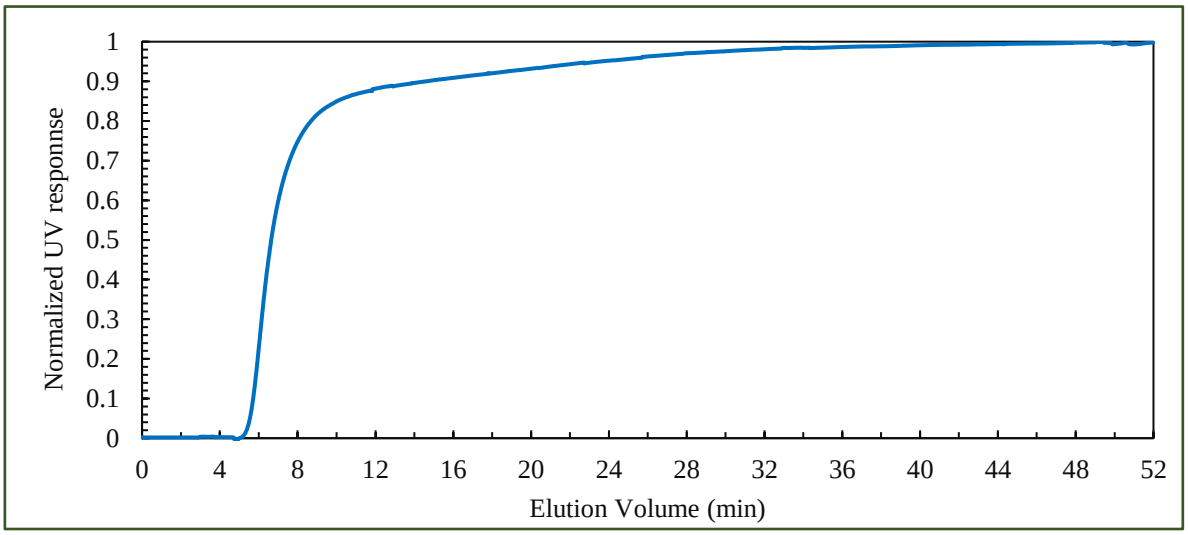

Graphic 13: Normalised breakthrough curve for the saturation of MIP7 on column using NATAC 70 in ethanol/water 90:10.

The results can also be presented as a function of the quantity eluted per quantity of mass of adsorbent. The study performed with MIP3, MIP12, DAX8 and REILLEX402, under the conditions presented in *Table 12* revealed better performance of MIP3 in relation to the others. These results reaffirm that the adsorbents synthesised based on 4VP (with/without molecular imprinting) have a good capacity to retain polyphenols present in olive leaf extracts. In particular, the high ability of the 4VP-based adsorbents to retain polyphenols even under conditions where there is little/no water is observed. The advantage of the 4VP adsorbents over commercial resins such as DAX8 is clear from the observation of the results presented in *Graphic 14***.**

Table 12: Specifications of the saturation procedure for the adsorbents MIP3, MIP12, DAX8 and Reillex402 in column with ethanol.

Material	Extract used	Solvent	Concentration (mg/mL)	Flow (mL/min)
MIP3	NATAC 70	Ethanol	0.22	1
MIP12	NATAC 70	Ethanol	0.22	1
DAX8	NATAC 70	Ethanol	0.22	1
REILLEX402	NATAC 70	Ethanol	0.22	1

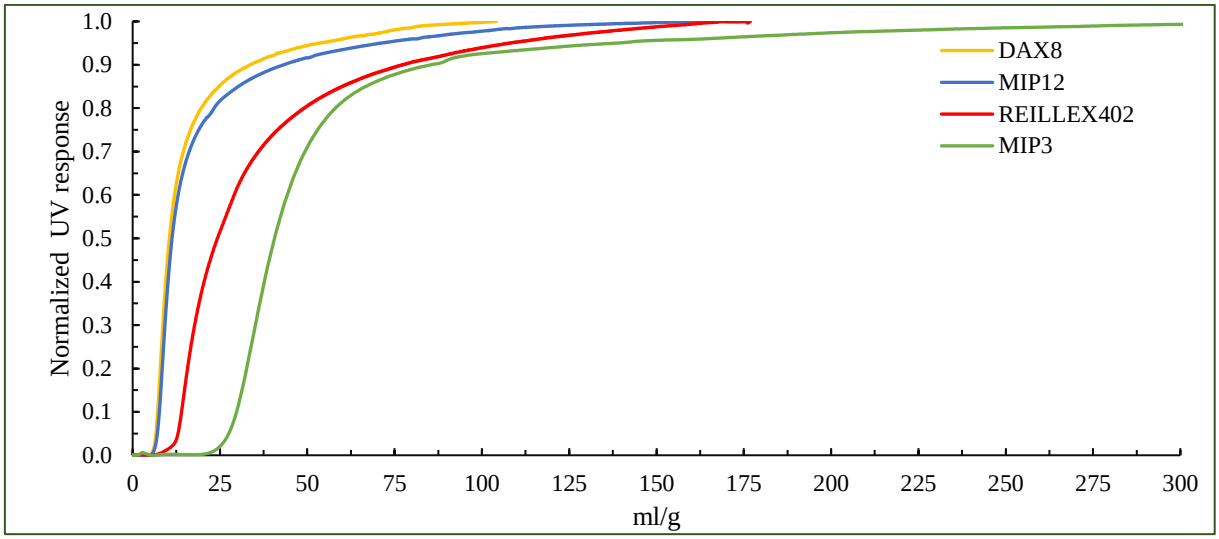

Graphic 14: Normalised breakthrough curve for the saturation of MIP3, MIP12, DAX8 and REILLEX402 in column using a 0.22 mg/mL solution of NATAC 70 in ethanol.

The next phase consisted in the desorption of the molecules retained in the packed materials, using different solvents in order to potentiate the fractionation of the compounds. This way, pre-established volumes of solvent were used and analysed firstly in UV-VIS, from this pre-evaluation, some fractions were selected for HPLC-DAD analysis. The specific conditions are described in *Table 13.*

Table 13: Specifications of the elution procedure for the adsorbents MIP3 and REILLEX402 in column.

Materials	Saturation conditions		Elution conditions		
	Extract	Solvent	Solvent	Temperature (°C)	Volume (mL)
MIP3	NATAC 20	Ethanol/water (90:10)	E1: Water	Room	3
			E2: Ethanol/Water 50:50	Room	3
			E3: Methanol	Room	3
			E4: Methanol/Acetic acid 90:10	Room	3
REILLEX402	NATAC 20	Ethanol/water (90:10)	E1: Water	45	30
			E2: Ethanol/Water 50:50	45	30
			E3: Ethanol/Water 90:10	45	30
			E4: Methanol	45	30
			E5: Methanol/Acetic acid 90:10	45	30

After UV-VIS readings of MIP3 elutions, fraction E3 was selected for further HPLC-DAD analysis, with this fraction, as seen in *Graphic 15*, a simplification of the initial extract is perceived, but there is no concentration of compounds relative to the initial extract.

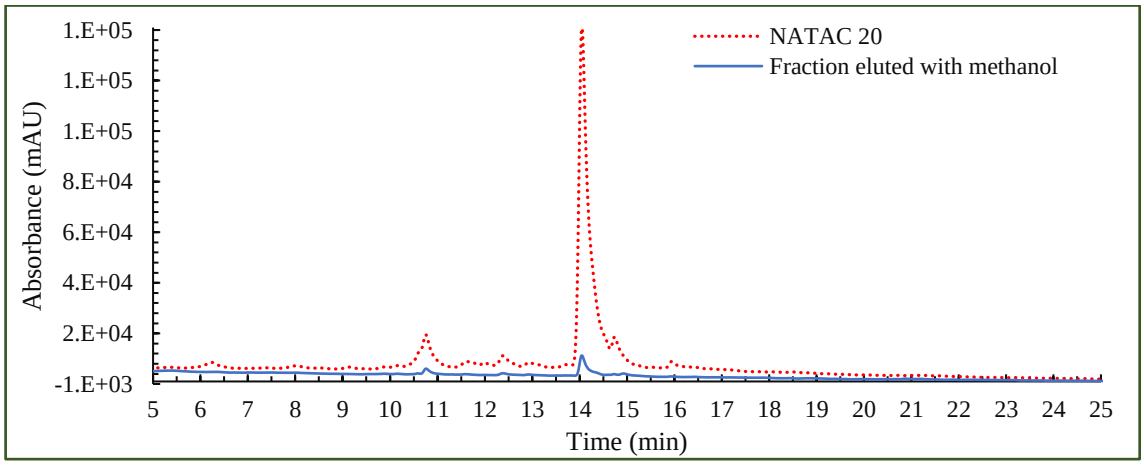

Graphic 15: HPLC-DAD analysis of NATAC 20 extract in ethanol/water 90:10 compared to the elution of MIP3 with methanol (E3) at room temperature. λ=255 nm.

As regards REILLEX402, with the first elution, E1, *Graphic 16*, between 5 and 10 min of retention it is observed a concentration of almost all the existing peaks. At 20 min there was the concentration of a peak relatively to the initial extract. With this fraction it was possible to identify luteolin-7-O-glucoside and verbascoside comparing the elution time and spectrum of the respective standards, as exemplified in *Graphics 52-54 seen in Appendix E.*

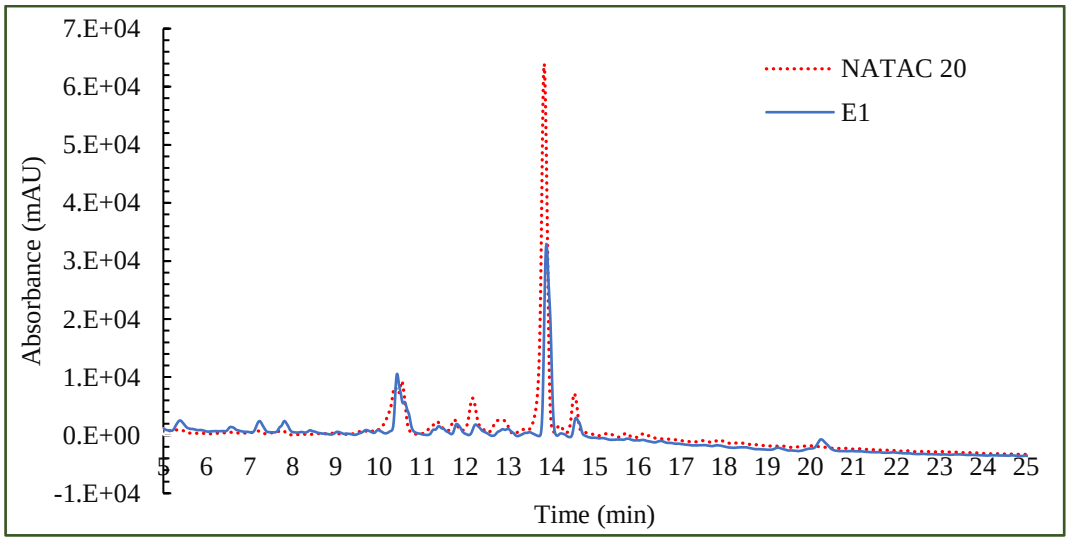

Graphic 16: HPLC-DAD analysis of NATAC 20 extract in ethanol/water 90:10 in comparison to the elution E1 (water) of REILLEX402. λ=280 nm.

In the next fraction, E2, *Graphic 17*, in general, concentration of the peaks with retention times at 7.9 min (a phenolic acid) and 10.6 min (luteolin-7-O-glucoside) was achieved. It was noted that the ratio between the luteolin and oleuropein peak is higher than in the initial extract (about 10x higher).

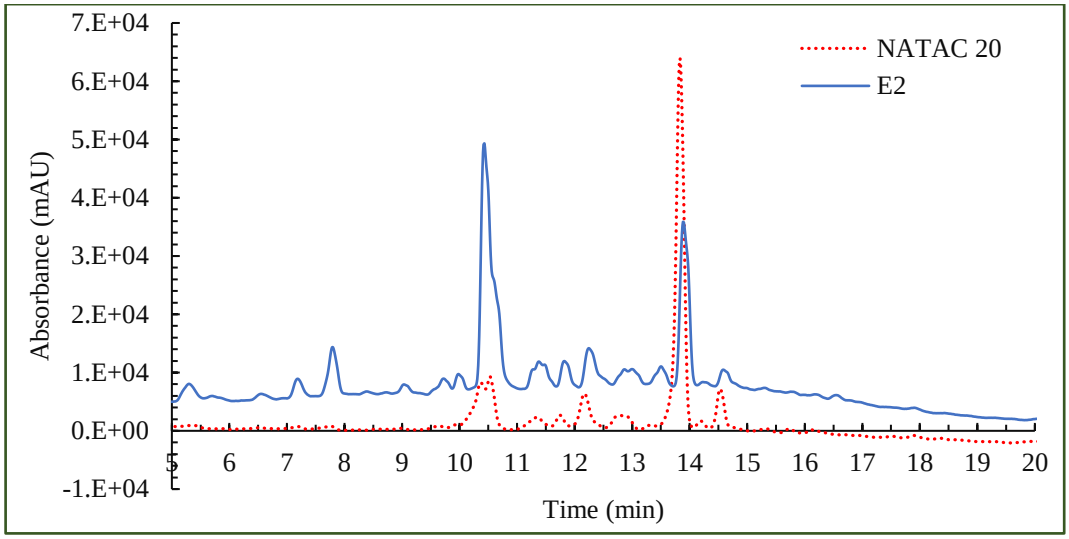

Graphic 17: HPLC-DAD analysis of NATAC 20 extract in ethanol/water 90:10 in comparison to the elution E2 (Ethanol/water 50:50) of REILLEX402. λ=280 nm.

In elution E3, *Graphic 18*, there was a great simplification of the initial extract, the peak corresponding to oleuropein was considerably reduced compared to the previous fractions. However, there was not a great concentration of the remaining peaks present in the extract. The majority peak corresponds to luteolin-7-O-glucoside at 10.6 min. In the same fraction at 10.4 min there is a peak whose spectrum and elution time corresponds to verbascoside.

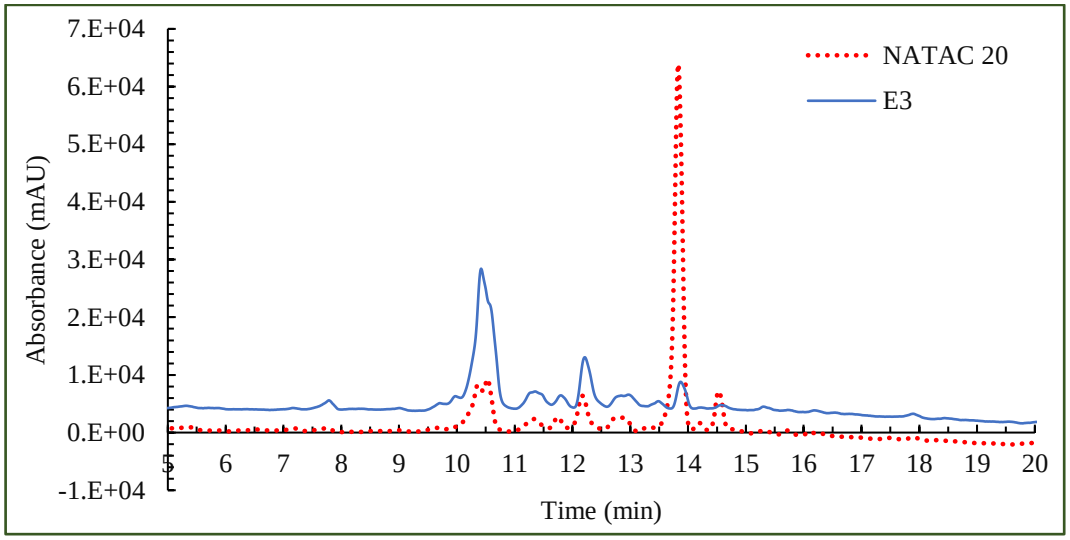

Graphic 18: HPLC-DAD analysis of NATAC 20 extract in ethanol/water 90:10 in comparison to the elution E3 (Ethanol/Water 90:10) of REILLEX402. λ=280 nm.

HPLC-DAD analysis of the next fraction, E4, *Graphic 19*, revealed very similar results to the previous fraction. The oleuropein peak is rather reduced and the luteolin-7-O-glucoside peak (10.6 min) appears somewhat more concentrated. It is evident that the peaks corresponding to luteolin-7-O-glucoside and verbascoside under the analysis conditions do not separate properly.

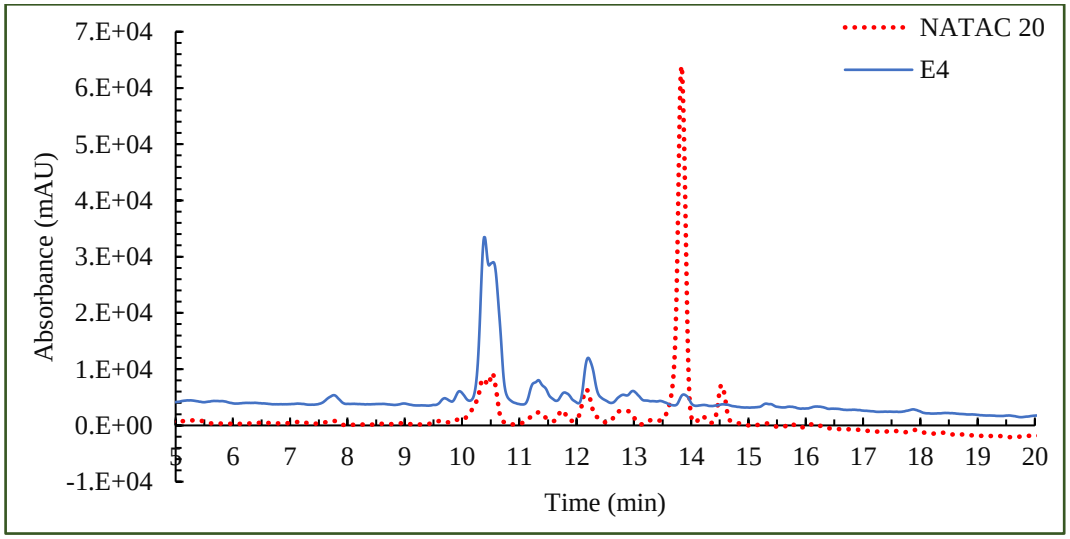

Graphic 19: HPLC-DAD analysis of NATAC 20 extract in ethanol/water 90:10 in comparison to the elution E4 (methanol) of REILLEX402. λ=280 nm.

The analysis of fraction E5, *Graphic 20*, showed a significant simplification in relation to the initial extract, in which a peak at 10.6 min is evidenced, whose spectrum and elution time correspond to luteolin-7-O-glucoside.

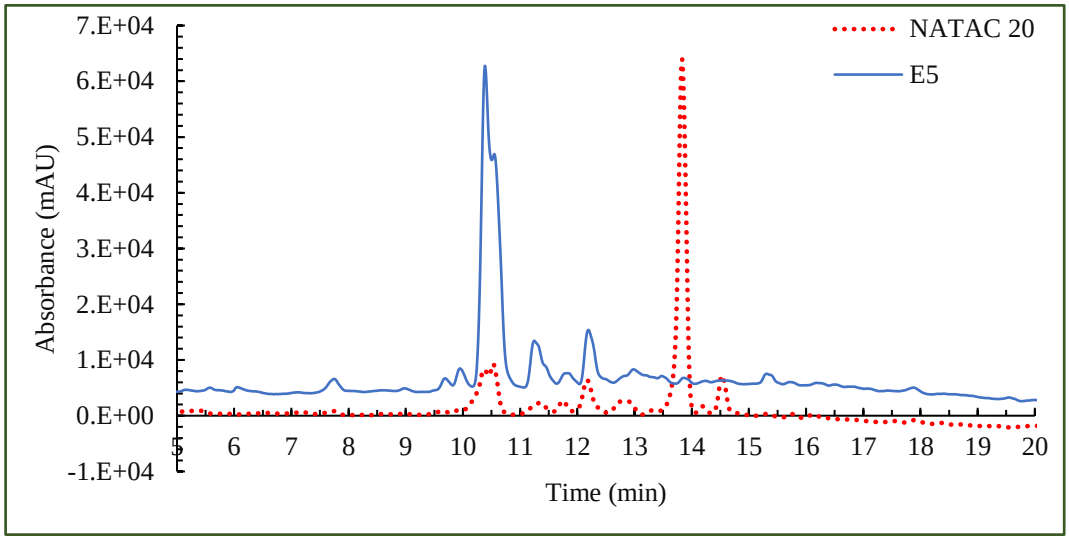

Graphic 20: HPLC-DAD analysis of NATAC 20 extract in ethanol/water 90:10 in comparison to the elution E5 (methanol/acetic acid 90:10) of REILLEX402. λ=280 nm.

CHAPTER 6. FINAL CONSIDERATIONS

It is imperative today to control the final application of residues, in the case of olive leaves, there is the possibility of aggregate value, since this residue is enriched in compounds that have increased value in the market. In this study, tailored materials that can selectively adsorb secoiridoids present in olive leaves were synthesized taking into consideration not only oleuropein, but also other families of phenolic compounds that are commonly found in olive leaf extracts. Besides the template, different morphological characteristics were explored by manipulating the parameters aforementioned. Polymerization by precipitation and by suspension were considered for this purpose. Based on previous studies in this field on 4-vinylpyridine, this monomer was inserted in a large part of the synthesized materials to enhance the interactions between pyridyl groups and the various polyphenols. The main objective of this study was to demonstrate the effect of molecular imprinting with oleuropein, so that its implementation in SPE systems was possible, aiming the fractionation and concentration of the compounds present in the extracts. As a way of comparison, commercial resins were also taken into consideration.

Using ultrasound and supercritical CO_2 extraction, extracts with different properties were generated in aqueous mixtures (ethanol/water) and also with pure solvents (ethyl acetate, CO_2). In contrast, extracts of know oleuropein percentage (NATAC 20, NATAC 40 and NATAC 70), resultants from the OLEAF4VALUE project were used, thus amplifying the alternatives for valorisation of these residues. The profile of each extract used was analysed by HPLC-DAD. FT-IR analysis of the produced materials showed the incorporation of the monomers in the final material and highlighted the amount of crosslinker used, which confers high stability to the final materials. Solid phase extraction was the first test performed to compare the adsorbents, these essays included oleuropein and vanillic acid, and by means of readings in UV-VIS the retention rates of both the synthesized adsorbents (MIP and NIP) and the commercial resins were determined.

The undertaken assays demonstrate the superior capacity of materials synthesized with 4-vinylpyridine to retain polyphenols contained in the various extracts used in this work. Again, with MIP3 and MIP7, the high polyphenol retention capacity of 4VP adsorbents is demonstrated. This is a consequence of the strong interaction between the pyridyl groups incorporated in these materials and the target molecules.

Through the study of the adsorption dynamics of polyphenols contained in the olive leaves, it was demonstrated the practical feasibility of using the 4VP adsorbents in continuous processes, more specifically in column and SPE operation. The SPE method with adsorbents synthesized with 4VP developed in this study, can be widely used in the easy, effective, and selective monitoring and analysis of the fractionation of olive leaf extracts, contributing to the valorisation of this residue. The Excellent stability and low-cost MIP, compared to NIP and a commercial adsorbent (REILLEX402) opens a window of opportunity for the potential industrial scalability of cyclic adsorption/desorption processes for concentration and fractionation of polyphenols present in the considered residues. The saturation curves presented reaffirm the behaviour of MIP3 in relation to the commercial resins used as well as the relevance of the interactions with the pyridyl group. The fractionation of the phenolic compounds was achieved with a sequence of elution in different solvents, being perceptible the enrichment in flavonoids in the organic and hydroalcoholic fractions, relatively to phenolic acids, and the identification of the phenolic compounds was made using the reference polyphenols. In parallel, with the NATAC 20 extract in ethanol/water (90/10) and the molecularly imprinted adsorbent MIP3, the simplification of the original phenolic profile was demonstrated.

It is suggested that further analysis of the molecular recognition ability (selectivity) of the adsorbents synthesized with 4VP (MIPs) relative to the non-imprinted analogues (NIPs) be carried out in the future. It is recommended that these studies are also carried out with extracts from extraction with supercritical CO_2. It is proposed that this study be supplemented by LC-DAD-ESI/MSn analyses for more rigorous identification of the polyphenols that might be fractionated and purified from the considered extracts.

CHAPTER 7. BIBLIOGRAPHIC REFERENCES

[1]. Santos, Luis. Ramos, António. A cultura da Oliveira. IPCB, Castelo Branco: Instituto Politécnico- Escola Superior Agrária de C. Branco. 1987.

[2]. Acar-Tek N., Ağagündüz D., Olive Leaf (Olea europaea L. folium): Potential Effects on Glycemia and Lipidemia. 2020, DOI: 10.1159/000505508, Annals of Nutrition and Metabolism. S. Karger AG, 2020. p. 10–5

[3]. Sedef N El, Karakaya S., Olive tree (Olea europaea) leaves: Potential beneficial effects on human health, Vol. 67, Nutrition Reviews, 2009, DOI: 10.1111/j.1753-4887.2009.00248.x, p. 632–8

[4]. Oliveira A.L.S., Gondim S., Gómez-García R., Ribeiro T., Pintado M., Olive leaf phenolic extract from two Portuguese cultivars –bioactivities for potential food and cosmetic application,. J Environ Chem Eng, 2021, doi.org/10.1016/j.jece.2021.106175

[5]. Kanti Bhooshan Pandey, Syed Ibrahim Rizvi. Plant polyphenols as dietary antioxidants in human health and disease, 2009, DOI: 10.4161/oxim.2.5.9498

[6]. Vogel P., Machado I.K., Garavaglia J., Zani V.T., D. de Souza, Dal Bosco, Beneficios polifenoles hoja de olivo (Olea europaea L) para la salud humana, Nutr Hosp, 2015, DOI:10.3305/nh.2015.31.3.8400

[7]. Barbaro B, Toietta G., Maggio R., Arciello M., Tarocchi M., Galli A., et al., Effects of the olive-derived polyphenol oleuropein on human health, Vol. 15, International Journal of Molecular Sciences, MDPI AG, 2014, DOI: 10.3390/ijms151018508

[8]. Omar S.H., Oleuropein in olive and its pharmacological effects, Vol. 78, Scientia Pharmaceutica, 2010, DOI: 10.3797/scipharm.0912-18, p. 133–54.

[9]. Otero D.M., Oliveira F.M., Lorini A., da Fonseca Antunes B, Oliveira RM, Zambiazi RC. Oleuropein: Methods for extraction, purifying and applying. Revista Ceres. 2020, DOI: 10.1590/0034-737x202067040009, 67(4):315–29.

[10]. Gomes C.P., Dias R.C.S., Costa M.R.P.F.N., Hybrid cellulose-poly(4-vinylpyridine) adsorbents produced via ATRP and their application to target polyphenols in winemaking, olive oil production and almond processing residues. React Funct Polym. 2021, DOI: 10.1016/j.reactfunctpolym.2021.104930, 164.

[11]. Wang Q., Shi A., Liu H., Liu L., Zhang Y., Li N., et al., Chapter 5 - Peanut By-Products Utilization Technology. In: Peanuts: Processing Technology and Product Development. Elsevier Inc., 2016, DOI: 10.1016/B978-0-12-809595-9.00005-3, p. 211–325.

[12]. Molecularly Imprinted Polymers in Biotechnology, Bo Mattiasson, Lei Ye Editors, 2015. p.2. ISBN: 978-3-319-20729-2

[13]. Molecularly Imprinted Polymers Man-made Mimics of Antibodies and their Applications in Analytical Chemistry. Edited by B.Sellergren. 2001. Vol. 23. ISBN-13: 978-0444828378

[14]. Alfred Rudin, The elements of polymer science and engineering, 2nd edition edition. 1998. ISBN 978-0-12-601685-7

[15]. Saldivar-Guerra Enrique, Vivaldo-Lima Eduardo, Handbook of Polymer Synthesis, Characterization, and Processing, John Wiley & Sons. 2013. ISBN 978-0-470-63032-7

[16]. Young, Robert J. Introduction to polymers. London: Chapman & Hall. 2nd editin.1991. ISBN 0-412-30640-9 (PB)
[17]. Odian, George. Principles of Polymerization. New York: John Wiley & Sons. 4th edition. 2004. ISBN 0-471-27400-3
[18]. Machado P.M.M., Cruz T.F., Bordado J.C., Gomes P.T., Controlled Radical Polymerization (ATRP and CMRP) of Vinyl Monomer Mediated by Cobalt (II/III) Complexes. 2015. Available at: https://fenix.tecnico.ulisboa.pt/downloadFile/563345090413925/Resumo%20Alargado.pdf. (Accessed November 12, 2022)
[19]. Prof. Rafique UI Islam. CHEM3020: Polymer Chemistry, Polymerization techniques. Motihari, Available at: https://mgcub.ac.in/pdf/material/20200405103131b1a374e0f3.pdf. (Accessed November 12, 2022)
[20]. He, C.Y., Long,Y.Y., Pan,J.L., Li, K. and Liu, F., Application of molecularly imprinted polymers to solid-phase extraction of analytes from real samples, Journal of Biochemical and Biophysical Methods, 2007, DOI: 10.1016/j.jbbm.2006.07.005, 70(2): p. 133-150
[21]. Gomes C.P., Franco V., Dias R.C.S., Costa M.R.P.F.N., Processing of Onion Skin Extracts with Quercetin-Molecularly Imprinted Adsorbents Working at a Wide Range of Water Content, Chromatographia, 2020, DOI: 10.1007/s10337-020-03958-0, 83(12):1539–51
[22]. Bo Mattiasson, Molecularly Imprinted Polymers in Biotechnology, Lei Ye Editors, p. 132
[23]. Sellergren B., Allender C.J., Molecularly imprinted polymers: A bridge to advanced drug delivery, Vol. 57, Advanced Drug Delivery Reviews, Elsevier, 2005, DOI: 10.1016/j.addr.2005.07.010, p. 1733–41.
[24]. Alves L. T. O., Erbetta C. D'Avila C., Fernandes C., et al.,. Síntese e caracterização de MIP com fenilalanina visando sua aplicação na técnica de SPE. Polímeros, 2015, DOI: 10.1590/0104-1428.2116, 25(6):596–605.
[25]. Suryyia Manzoor. Materiais Impressos Molecularmente (MIMs): Síntese, Caracterização e Avaliação, Campinas, 2013, Available at: https://bdtd.ibict.br/vufind/Record/CAMP_bfa551f28216aef0129d543c94f7861f
[26]. Sousa M.D., Maurício B.C., Polímeros com Capacidade de Reconhecimento Molecular no Controlo da Libertação de Fármacos. Parte 1: Síntese e Caracterização, Vol. 32, Quim. Nova, 2009, DOI: 10.1590/S0100-40422009000600045
[27]. Hasanah A.N., Safitri N., Zulfa A., Neli N., Rahayu D., Factors affecting preparation of molecularly imprinted polymer and methods on finding template-monomer interaction as the key of selective properties of the materials, Vol. 26, Molecules, MDPI, 2021, DOI: 10.3390/molecules26185612
[28]. Yan H., Ho Row K., Characteristic and Synthetic Approach of Molecularly Imprinted Polymer, Int J Mol Sci, 2006, ISSN: 1422-0067, 7:155–78, Available at: www.mdpi.org/ijms/
[29]. Cormack P.A.G., Elorza A.Z., Molecularly imprinted polymers: Synthesis and characterisation, Vol. 804, Journal of Chromatography B: Analytical Technologies in the Biomedical and Life Sciences, 2004, DOI: 10.1016/j.jchromb.2004.02.013, p. 173–82.

[30]. Madikizela L.M., Nomngongo P.N., Pakade V.E., Synthesis of molecularly imprinted polymers for extraction of fluoroquinolones in environmental, food and biological samples, Vol. 208, Journal of Pharmaceutical and Biomedical Analysis. Elsevier B.V., 2022, DOI: 10.1016/j.jpba.2021.114447

[31]. Hermawan B.A., Mutakin, Hasanah A.N., Role of porogenic solvent type on the performance of a monolithic imprinted column, Vol. 75, Chemical Paper. Springer Science and Business Media Deutschland GmbH, 2020, DOI: 10.1007/s11696-020-01399-5, p. 1301–11

[32]. Jaraiseh H., Afaneh I., Al-Rimawi F., Optimum Conditions for Oleuropein Extraction from Olive Leaves, Vol. 4, International Journal of Applied Science and Technology, 2014, Available at: https://www.researchgate.net/publication/271014114

[33]. Coppa C.F.S.C., Rosim R.E., Oliveira C. A. F., et al., Extração de oleuropeína a partir de folhas de oliveira utilizando solvente hidroalcoólico. Vol. 20, Brazilian Journal of Food Technology, Instituto de Tecnologia de Alimentos – ITAL, 2017, DOI: 10.1590/1981-6723.16916

[34]. Didaskalou C., Buyuktiryaki S., Kecili R., Claudio P. Fonte, Szekely G., Valorisation of agricultural waste with an adsorption/nanofiltration hybrid process: from materials to sustainable process design, 2017, DOI: 10.1039/c7gc00912g

[35]. Gomes C.P., Dias R.C.S., Costa M.R.P.F.N., Preparation of Molecularly Imprinted Adsorbents with Improved Retention Capability of Polyphenols and Their Application in Continuous Separation Processes, Chromatographia 82, 893–916 (2019), DOI: https://doi.org/10.1007/s10337-019-03728-7

[36]. D. Oliveira, C.P. Gomes, R.C.S. Dias, M.R.P.F.N. Costa, Molecular imprinting of 5-fluorouracil in particles with surface RAFT grafted functional brushes, 2016, DOI: https://doi.org/10.1016/j.reactfunctpolym.2016.08.007

[37]. Gomes C.P., Sadoyan G., Dias R.C.S., Mário Rui P. F. N. Costa, Development of Molecularly Imprinted Polymers to Target Polyphenols Present in Plant Extracts, 2017, DOI: https://doi.org/10.3390/pr5040072

[38]. Amir Bzainia, Rolando C. S. Dias, Mário Rui P. F. N. Costa, Enrichment of Quercetin from Winemaking Residual Diatomaceous Earth via a Tailor-Made Imprinted Adsorbent, 2022, DOI: https://doi.org/10.3390/molecules27196406

[39]. A. Marffn-Esteban, E. TurieP, D. Stevenson, Effect of Template Size on the Selectivity of Molecularly Imprinted Polymers for Phenylurea Herbicides, Chromatographia Supplement Vol. 53, 2001, DOI: 10.1007/BF02490371

Appendix

Appendix A: HPLC-DAD analysis of the phenolic profile of the different extracts used in this work.

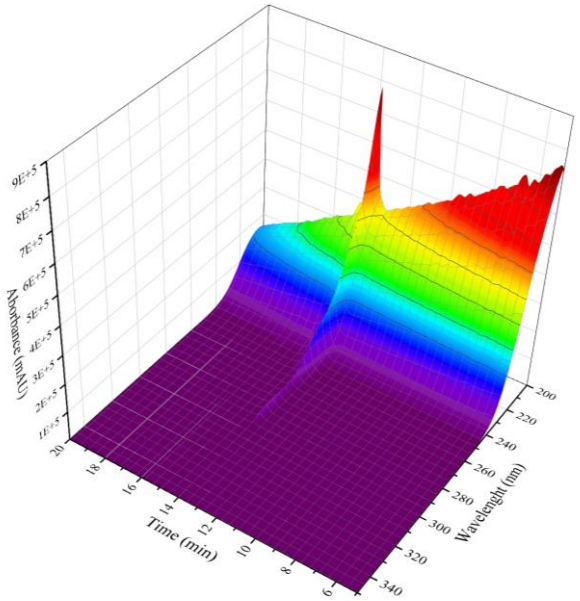

Figure 33: HPLC-DAD analysis of the extract obtained from the Madural leaves variety, extracted with ethyl acetate, injected in acetonitrile (MA1).

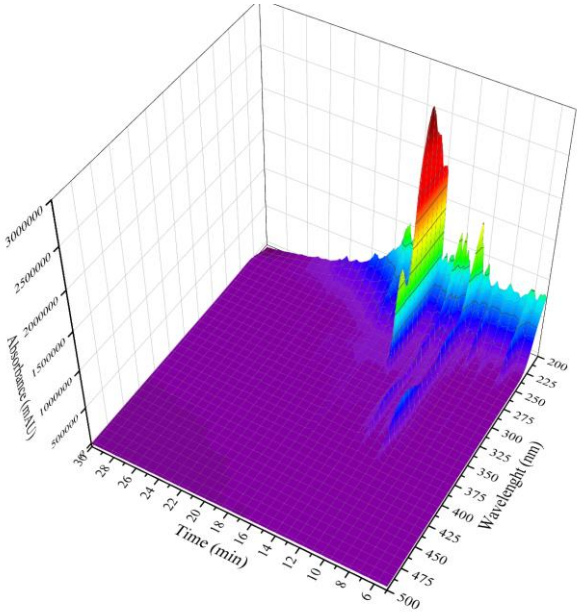

Figure 34: HPLC-DAD analysis of the extract obtained from the Madural leaves variety, extracted with ethanol/water 80:20, injected in ethanol/water 80:20 (MA2).

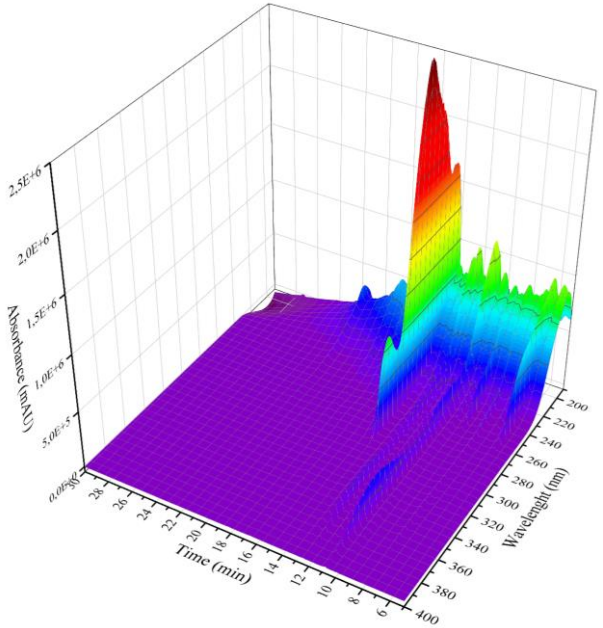

Figure 35: HPLC-DAD analysis of the extract obtained from the Madural leaves variety, extracted with ethanol/water 50:50, injected in ethanol/water 50:50 (MA3).

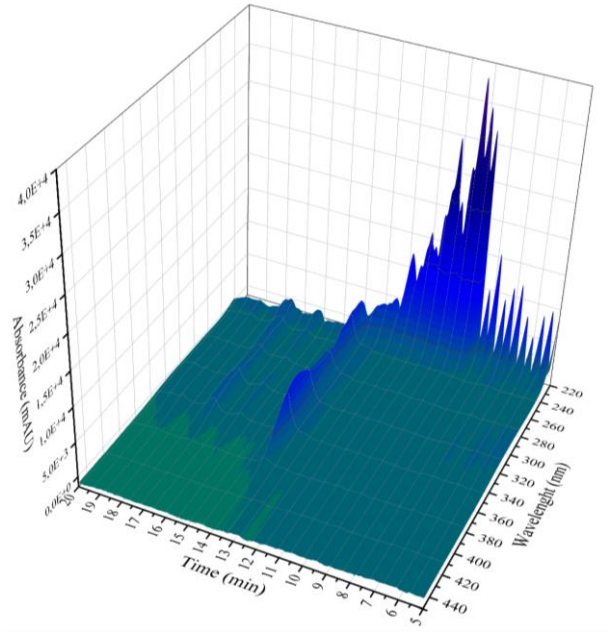

Figure 36: HPLC-DAD analysis of the extract NATAC20, injected in ethanol/water 90:10 at 0.5 mg/mL.

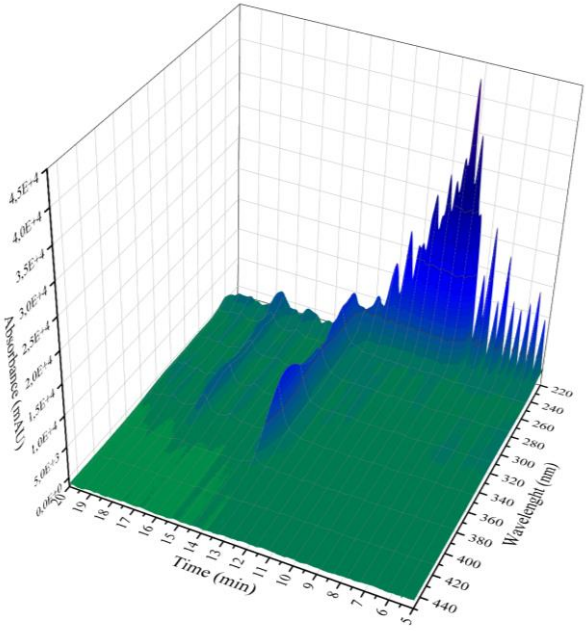

Figure 37: HPLC-DAD analysis of the extract NATAC40, injected in ethanol/water 90:10 at 0.5 mg/mL.

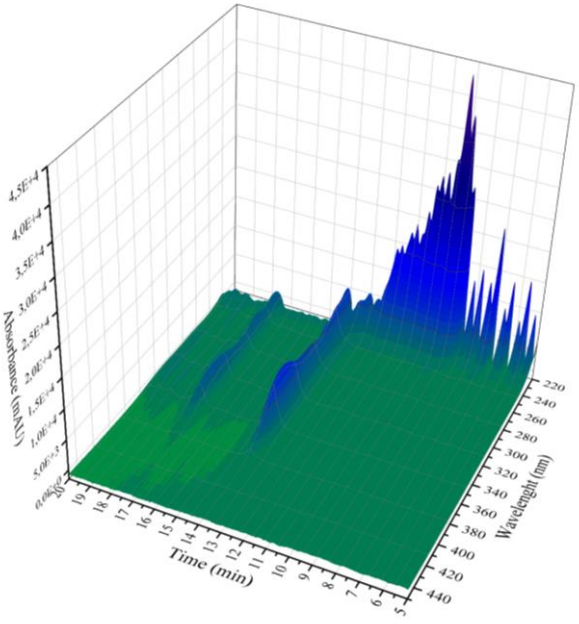

Figure 38: HPLC-DAD analysis of the extract NATAC70, injected in ethanol/water 90:10 at 0.5 mg/mL.

Appendix B: HPLC-DAD analysis of the standards considered in this work for comparison with the phenolic profile observed in olive leaf extracts.

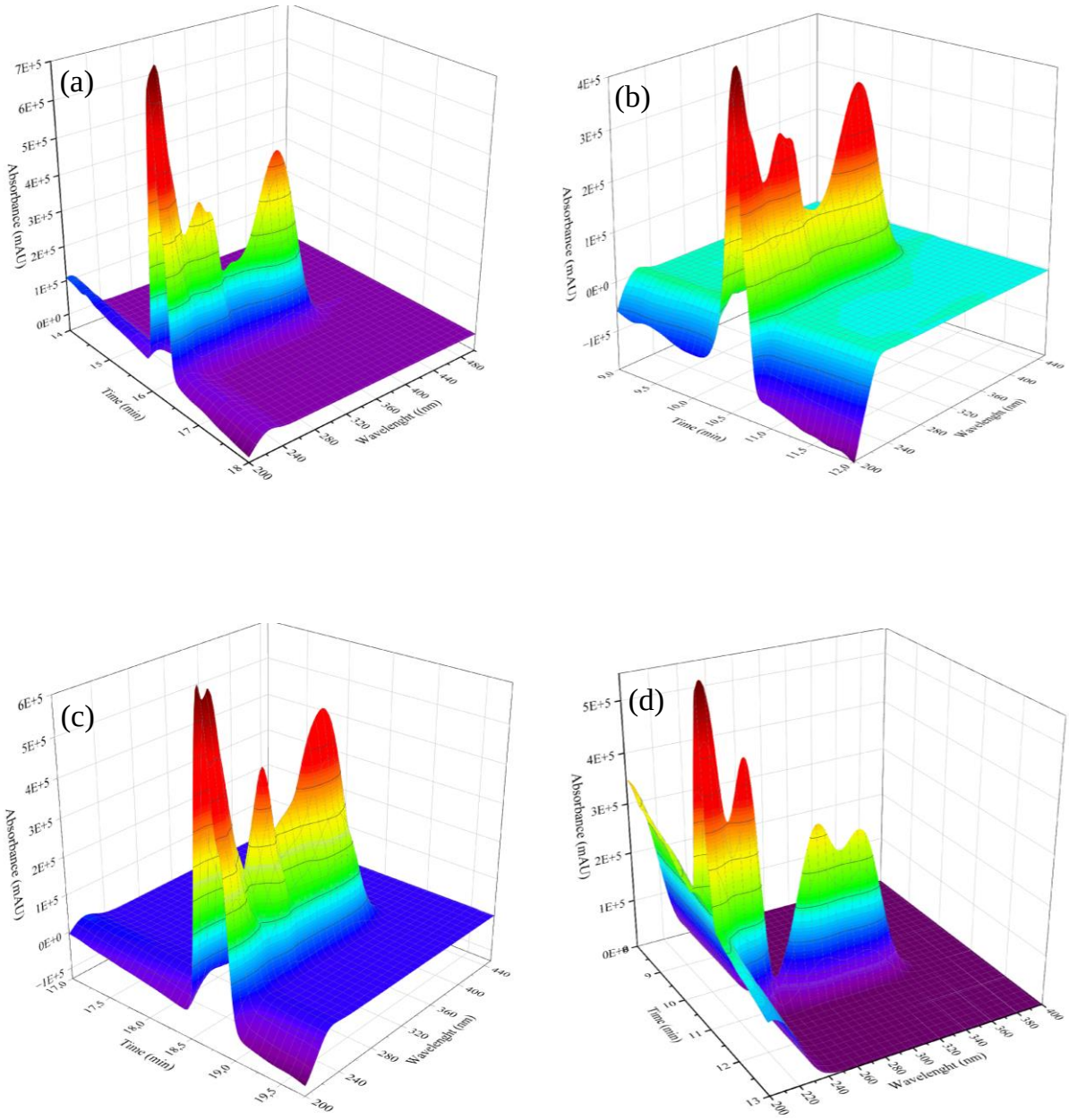

Figure 39: HPLC-DAD analysis of standards for comparison with the phenolic profile observed in olive leaf extracts. (a): Luteolin. (b): Luteolin-7-O-Glucoside. (c): Apigenin. (d): Vanillin.

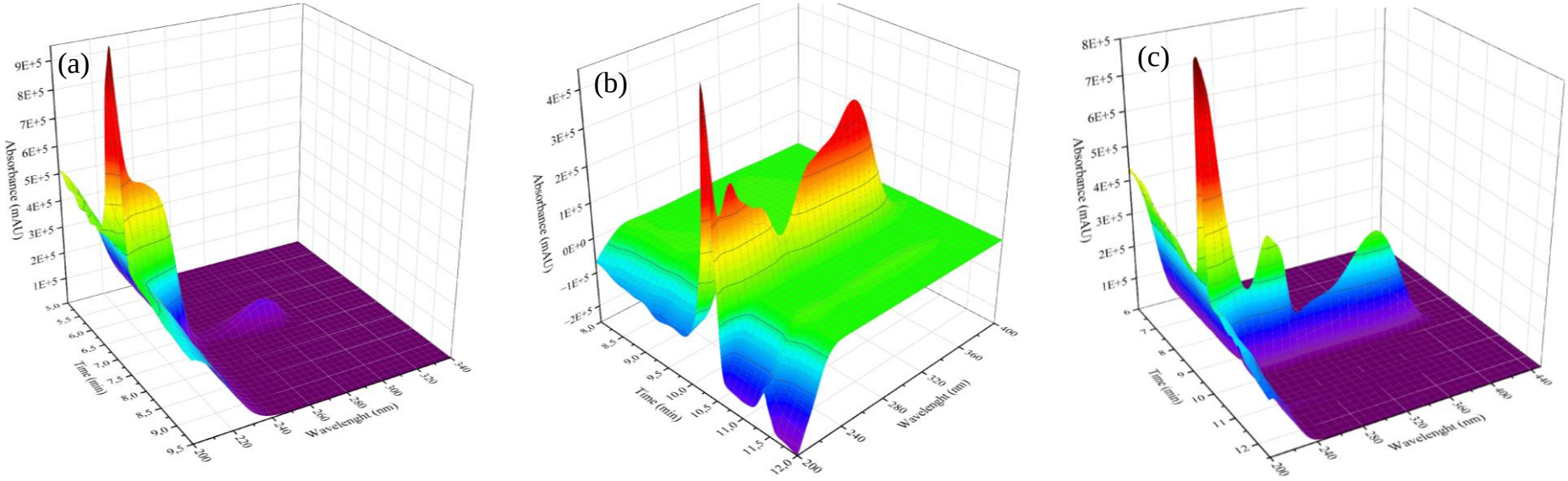

Figure 40:HPLC-DAD analysis of standards for comparison with the phenolic profile observed in olive leaf extracts. (a): Tyrosol. (b): Verbascoside. (c): Rutin.

Appendix C: FT-IR spectrum of molecularly imprinted polymer in contrast to corresponding functional monomers and crosslinker.

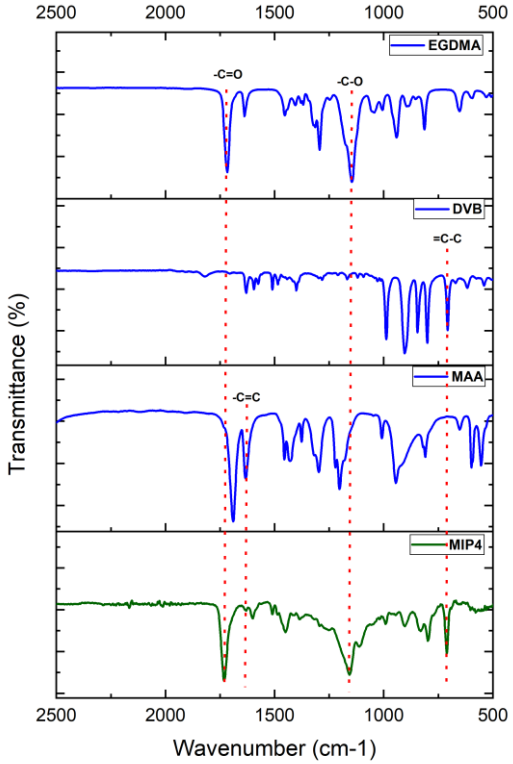

Figure 41: FT-IR spectrum of MIP4 in contrast to the corresponding functional monomers (MAA, DVB) and the crosslinker (EGDMA).

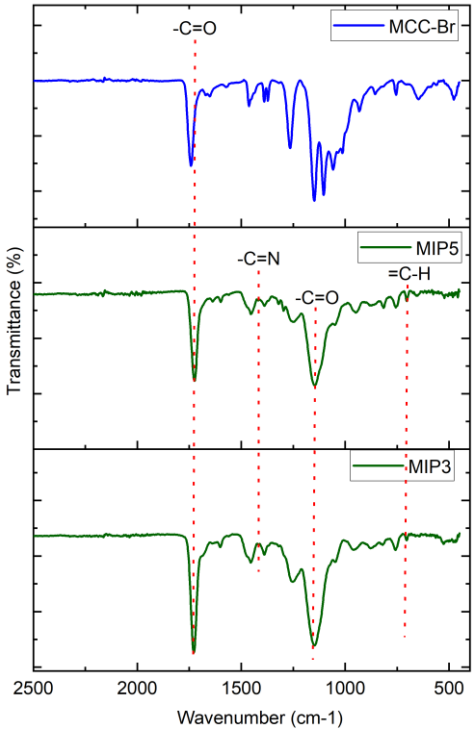

Figure 42: FT-IR spectrum of MIP3 and MIP5 in contrast to the macro initiator (MCC-Br).

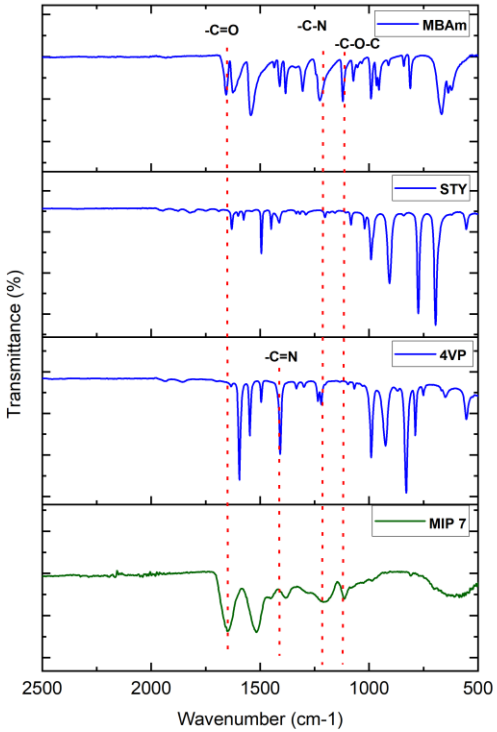

Figure 43: FT-IR spectrum of MIP7 in contrast to the corresponding functional monomers (4VP, STY) and the crosslinker (MBAm)

Appendix D: Graphical demonstration of competitive retention during adsorption.

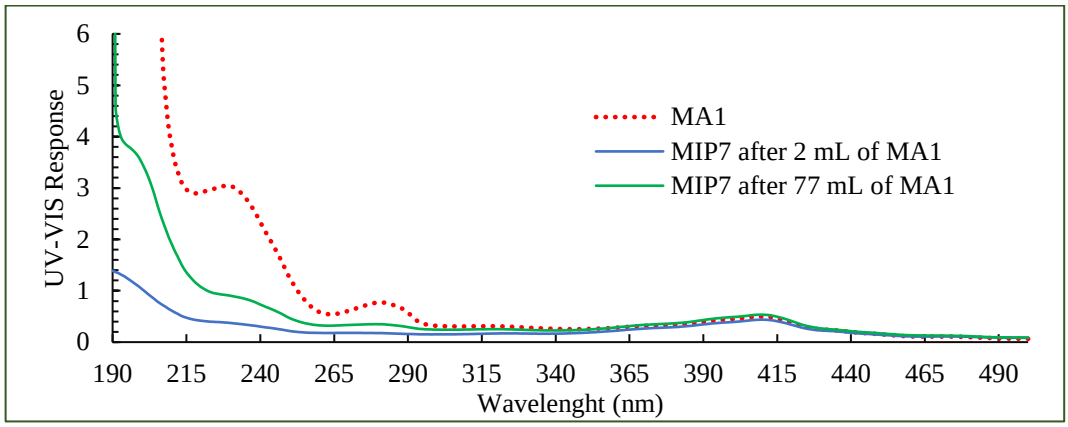

Graphic 21: UV-VIS Chromatogram comparison of the initial extract MA1 (ACN, 0.2 mg/mL) with fractions collected after passing 2, and 77 mL through MIP7.

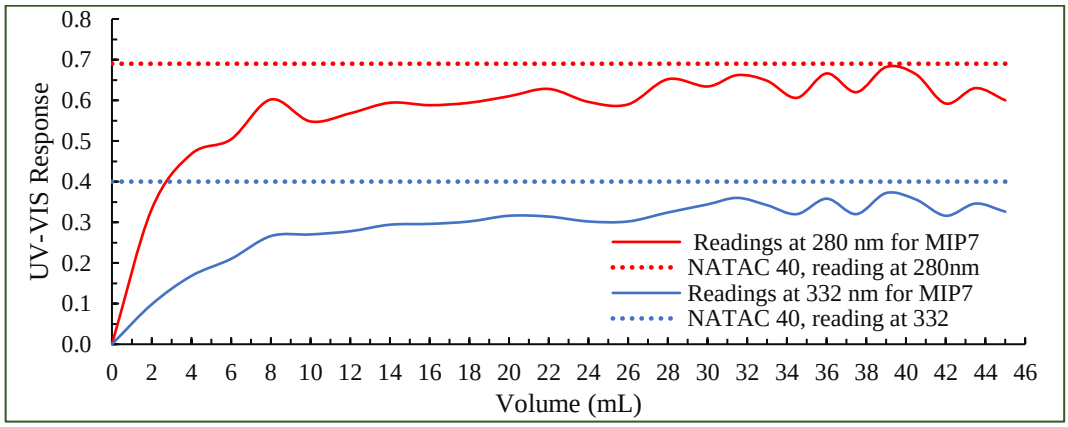

Graphic 22: Saturation curve of MIP7 in comparison with the initial response of the extract NATAC 40 in ethanol/water 90:10 (0.1 mg/mL) at the wavelengths 280 and 332 nm.

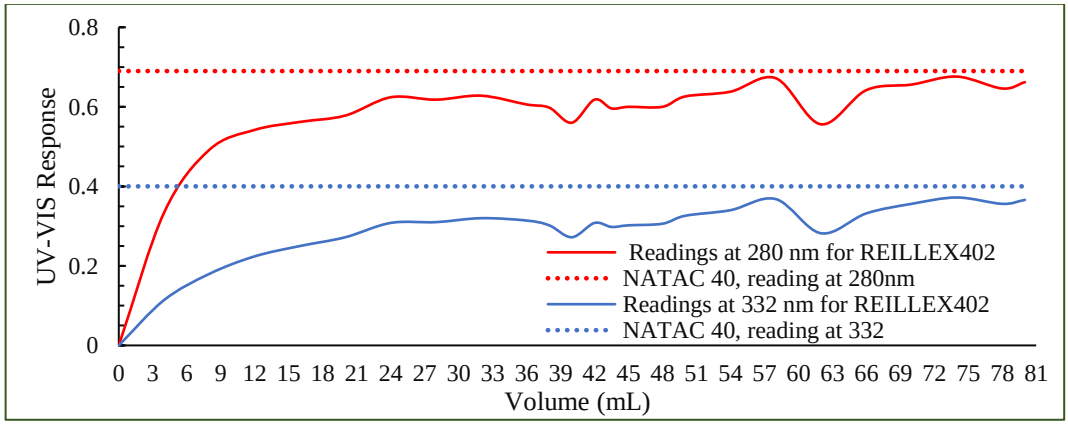

Graphic 23: Saturation curve of MIP7 in comparison with the initial response of the extract NATAC 40 in ethanol/water 90:10 (0.1 mg/mL) at the wavelengths 280 and 332 nm.

Appendix E: Identification of the peaks found in extracts/elution fractions using HPLC-DAD analysis by comparison with injected standards.

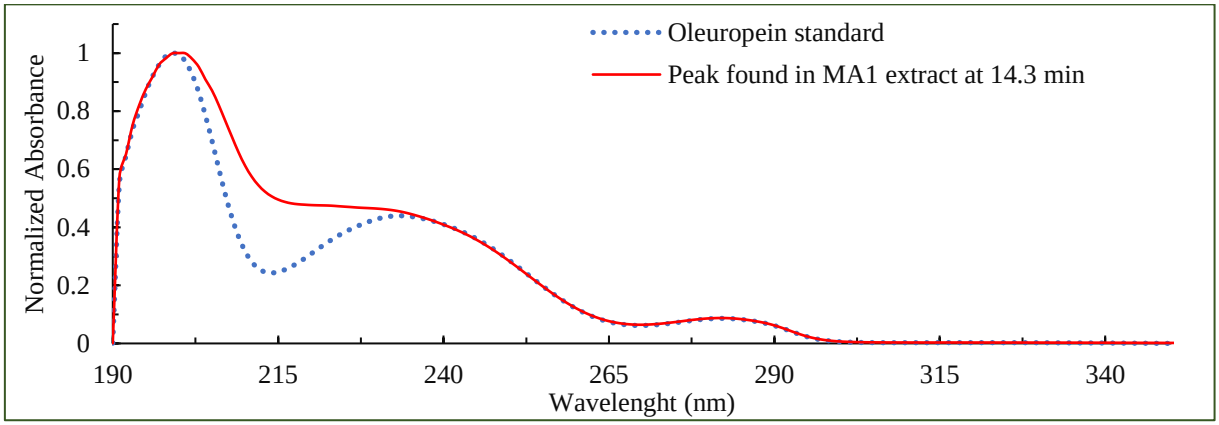

Graphic 24: Identification of Oleuropein in MA1 extract via HPLC-DAD chromatogram comparison. Elution time of oleuropein standard is 14.3 min.

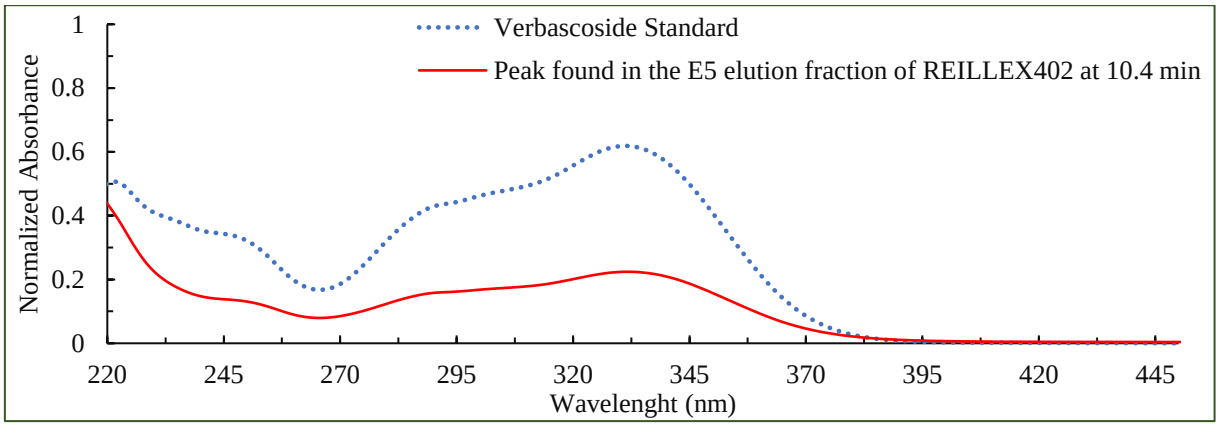

Graphic 25: Identification of Verbascoside in the elution of REILLEX402 with methanol/acetic acid 90:10 (E5) via HPLC-DAD chromatogram comparison. Elution time of verbascoside standard is 10.4 min.

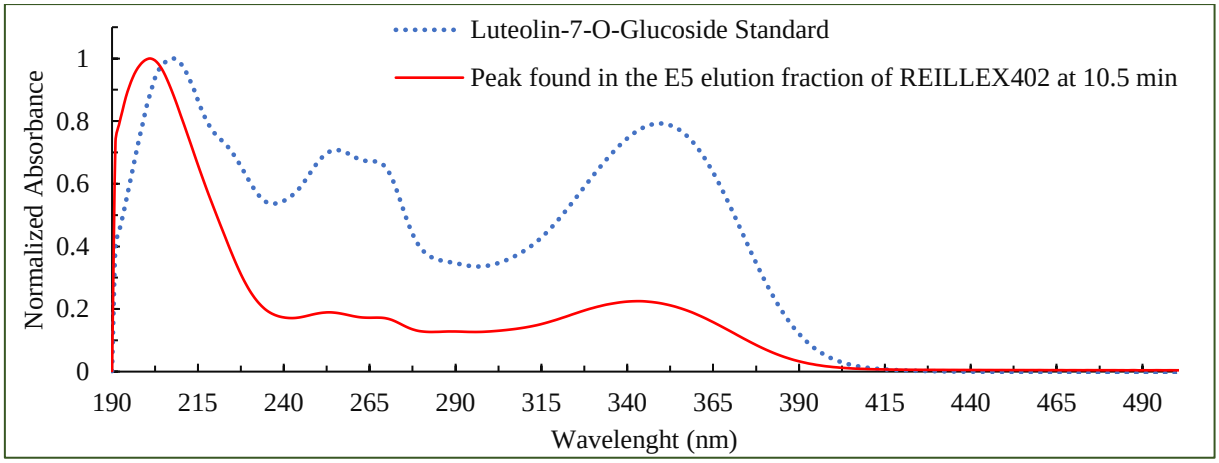

Graphic 26: Identification of Luteolin-7-O-Glucoside in the elution of REILLEX402 with methanol/acetic acid 90:10 (E5) via HPLC-DAD chromatogram comparison. Elution time of Luteolin-7-O-Glucoside standard is 10.5 min.